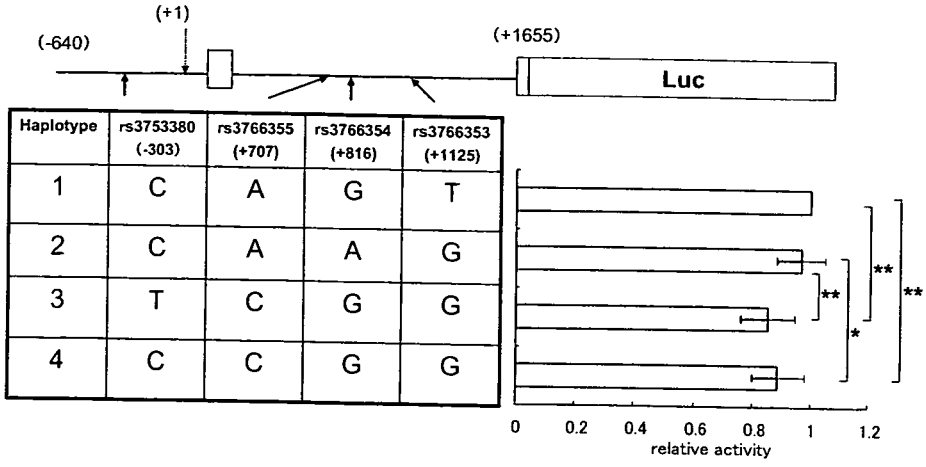

Figure 2. Effects of 4 haplotype combinations of 4 single-nucleotide polymorphisms (SNPs) on the transcriptional activity of the prostaglandin $F_{2\alpha}$ receptor gene. Top, Structure of the reporter gene construct and the position of each SNP. Luc = firefly luciferase gene. Bottom, The haplotype combination of each clone and relative luciferase activity. Luciferase activity was divided by the activity of renilla to normalize transfection efficiency. Relative activity was calculated with the value of haplotype 1 being 1.0. The values represent means ± standard deviations from 15 independent experiments. Student's *t* tests were performed on paired samples. *$P<0.02$. **$P<0.01$.

In conclusion, we found an association between 2 SNPs, rs3753380 and rs3766355, in the promoter and intron 1 regions of the FP receptor gene and a short-term latanoprost response in healthy volunteers. The results of the promoter assay suggest that these SNPs downregulate expression of the FP receptor gene, resulting in diminished IOP reduction by latanoprost. Because this study examined only the short-term (1 week) effect of latanoprost in normal subjects, long-term results in patients with glaucoma or ocular hypertension are needed to clarify further the significance of these SNPs in the IOP-lowering effect by latanoprost. Nevertheless, the genotype of these SNPs may be an important determinant of variability in response to latanoprost.

References

1. Aung T, Chew PT, Yip CC, et al. A randomized double-masked crossover study comparing latanoprost 0.005% with unoprostone 0.12% in patients with primary open-angle glaucoma and ocular hypertension. Am J Ophthalmol 2001;131: 636–42.
2. Scherer WJ. A retrospective review of non-responders to latanoprost. J Ocul Pharmacol Ther 2002;18:287–91.
3. Sofowora GG, Dishy V, Muszkat M, et al. A common beta1-adrenergic receptor polymorphism (Arg389Gly) affects blood pressure response to beta-blockade. Clin Pharmacol Ther 2003;73:366–71.
4. Brodde OE, Stein CM. The Gly389Arg beta1-adrenergic receptor polymorphism: a predictor of response to beta-blocker treatment? Clin Pharmacol Ther 2003;74:299–302.
5. Martinez FD, Graves PE, Baldini M, et al. Association between genetic polymorphisms of the beta2-adrenoceptor and response to albuterol in children with and without a history of wheezing. J Clin Invest 1997;100:3184–8.
6. Evans WE, McLeod HL. Pharmacogenomics—drug disposition, drug targets, and side effects. N Engl J Med 2003;348: 538–49.
7. Sasaki M, Oki T, Iuchi A, et al. Relationship between the angiotensin converting enzyme gene polymorphism and the effects of enalapril on left ventricular hypertrophy and impaired diastolic filling in essential hypertension: M-mode and pulsed Doppler echocardiographic studies. J Hypertens 1996;14:1403–8.
8. Baudin B. Angiotensin II receptor polymorphisms in hypertension: pharmacogenomic considerations. Pharmacogenomics 2002;3:65–73.
9. Miller JA, Thai K, Scholey JW. Angiotensin II type 1 receptor gene polymorphism predicts response to losartan and angiotensin II. Kidney Int 1999;56:2173–80.
10. Schwartz SG, Puckett BJ, Allen RC, et al. β_1-adrenergic receptor polymorphisms and clinical efficacy of betaxolol hydrochloride in normal volunteers. Ophthalmology 2005; 112:2131–6.
11. Stjernschantz J, Selen G, Sjoquist B, Resul B. Preclinical pharmacology of latanoprost, a phenyl-substituted PGF2 alpha analogue. Adv Prostaglandin Thromboxane Leukot Res 1995; 23:513–8.
12. Abramovitz M, Boie Y, Nguyen T, et al. Cloning and expression of a cDNA for the human prostanoid FP receptor. J Biol Chem 1994;269:2632–6.
13. Betz R, Lagercrantz J, Kedra D, et al. Genomic structure, 5′ flanking sequences, and precise localization in 1P31.1 of the human prostaglandin F receptor gene. Biochem Biophys Res Commun 1999;254:413–6.
14. Vielhauer GA, Fujino H, Regan JW. Cloning and localization of hFP(S): a six-transmembrane mRNA splice variant of the human FP prostanoid receptor. Arch Biochem Biophys 2004; 421:175–85.
15. Ocklind A, Lake S, Wentzel P, et al. Localization of the prostaglandin F2 alpha receptor messenger RNA and protein in the cynomolgus monkey eye. Invest Ophthalmol Vis Sci 1996;37:716–26.
16. Schlotzer-Schrehardt U, Zenkel M, Nusing RM. Expression and localization of FP and EP prostanoid receptor subtypes in human ocular tissues. Invest Ophthalmol Vis Sci 2002;43: 1475–87.
17. Mukhopadhyay P, Bian L, Yin H, et al. Localization of EP(1) and FP receptors in human ocular tissues by in situ hybridization. Invest Ophthalmol Vis Sci 2001;42:424–8.
18. Watanabe T, Nakao A, Emerling D, et al. Prostaglandin F2 alpha enhances tyrosine phosphorylation and DNA synthe-

sis through phospholipase C-coupled receptor via Ca(2+)-dependent intracellular pathway in NIH-3T3 cells. J Biol Chem 1994;269:17619–25.
19. Sugimoto Y, Hasumoto K, Namba T, et al. Cloning and expression of a cDNA for mouse prostaglandin F receptor. J Biol Chem 1994;269:1356–60.
20. Weinreb RN, Kashiwagi K, Kashiwagi F, et al. Prostaglandins increase matrix metalloproteinase release from human ciliary smooth muscle cells. Invest Ophthalmol Vis Sci 1997;38: 2772–80.
21. Gaton DD, Sagara T, Lindsey JD, et al. Increased matrix metalloproteinases 1, 2, and 3 in the monkey uveoscleral outflow pathway after topical prostaglandin F(2 alpha)-isopropyl ester treatment. Arch Ophthalmol 2001;119: 1165–70.
22. Weinreb RN, Lindsey JD. Metalloproteinase gene transcription in human ciliary muscle cells with latanoprost. Invest Ophthalmol Vis Sci 2002;43:716–22.
23. Lindsey JD, Kashiwagi K, Kashiwagi F, Weinreb RN. Prostaglandins alter extracellular matrix adjacent to human ciliary muscle cells in vitro. Invest Ophthalmol Vis Sci 1997;38: 2214–23.
24. Ocklind A. Effect of latanoprost on the extracellular matrix of the ciliary muscle: a study on cultured cells and tissue sections. Exp Eye Res 1998;67:179–91.
25. Toris CB, Camras CB, Yablonski ME. Effects of PhXA41, a new prostaglandin F2 alpha analog, on aqueous humor dynamics in human eyes. Ophthalmology 1993;100:1297–304.
26. Crowston JG, Lindsey JD, Aihara M, Weinreb RN. Effect of latanoprost on intraocular pressure in mice lacking prostaglandin FP receptor. Invest Ophthalmol Vis Sci 2004;45:3555–9.
27. Zaragoza DB, Wilson R, Eyster K, Olson DM. Cloning and characterization of the promoter region of the human prostaglandin F2alpha receptor gene. Biochim Biophys Acta 2004; 1676:193–202.
28. Excoffier L, Slatkin M. Maximum-likelihood estimation of molecular haplotype frequencies in a diploid population. Mol Biol Evol 1995;12:921–7.
29. Stjernschantz JW. From PGF(2alpha)-isopropyl ester to latanoprost: a review of the development of xalatan. The Proctor Lecture. Invest Ophthalmol Vis Sci 2001;42: 1134–45.
30. Rulo AH, Greve EL, Geijssen HC, Hoyng PF. Reduction of intraocular pressure with treatment of latanoprost once daily in patients with normal-pressure glaucoma. Ophthalmology 1996;103:1276–82.
31. Tamada Y, Taniguchi T, Murase H, et al. Intraocular pressure-lowering efficacy of latanoprost in patients with normal-tension glaucoma or primary open-angle glaucoma. J Ocul Pharmacol Ther 2001;17:19–25.
32. Ezashi T, Sakamoto K, Miwa K, et al. Genomic organization and characterization of the gene encoding bovine prostaglandin F2alpha receptor. Gene 1997;190:271–8.
33. Neuschafer-Rube F, Moller U, Puschel GP. Structure of the 5′-flanking region of the rat prostaglandin F(2alpha) receptor gene and its transcriptional control functions in hepatocytes. Biochem Biophys Res Commun 2000;278:278–85.
34. Neuschafer-Rube F, Engemaier E, Koch S, et al. Identification by site-directed mutagenesis of amino acids contributing to ligand-binding specificity or signal transduction properties of the human FP prostanoid receptor. Biochem J 2003;371: 443–9.
35. Maxey KM, Johnson JL, LaBrecque J. The hydrolysis of bimatoprost in corneal tissue generates a potent prostanoid FP receptor agonist. Surv Ophthalmol 2002;47(suppl):S34–40.
36. Orlicky DJ. Negative regulatory activity of a prostaglandin F2 alpha receptor associated protein (FPRP). Prostaglandins Leukot Essent Fatty Acids 1996;54:247–59.
37. Van Der Zwaag B, Verzijl HT, Beltran-Valero de Bernabe D, et al. Mutation analysis in the candidate Mobius syndrome genes *PGT* and *GATA2* on chromosome 3 and *EGR2* on chromosome 10 [letter online]. J Med Genet 2002;39:E30. Available at http://jmg.bmjjournals.com/cgi/content/full/39/6/e30. Accessed June 30, 2002.
38. Sipe JC, Chiang K, Gerber AL, et al. A missense mutation in human fatty acid amide hydrolase associated with problem drug use. Proc Natl Acad Sci U S A 2002;99:8394–9.
39. Rutter JL, Mitchell TI, Buttice G, et al. A single nucleotide polymorphism in the matrix metalloproteinase-1 promoter creates an Ets binding site and augments transcription. Cancer Res 1998;58:5321–5.
40. Price SJ, Greaves DR, Watkins H. Identification of novel, functional genetic variants in the human matrix metalloproteinase-2 gene: role of Sp1 in allele-specific transcriptional regulation. J Biol Chem 2001;276:7549–58.
41. Ye S, Watts GF, Mandalia S, et al. Preliminary report: genetic variation in the human stromelysin promoter is associated with progression of coronary atherosclerosis. Br Heart J 1995;73: 209–15.
42. Zhang B, Ye S, Herrmann SM, et al. Functional polymorphism in the regulatory region of gelatinase B gene in relation to severity of coronary atherosclerosis. Circulation 1999;99:1788–94.
43. St Jean PL, Zhang XC, Hart BK, et al. Characterization of a dinucleotide repeat in the 92 kDa type IV collagenase gene (*CLG4B*), localization of *CLG4B* to chromosome 20 and the role of *CLG4B* in aortic aneurysmal disease. Ann Hum Genet 1995;59:17–24.

JOURNAL OF OCULAR PHARMACOLOGY AND THERAPEUTICS
Volume 22, Number 6, 2006

The Inhibitory Effect of Nilvadipine on Calcium Channels in Retinal Ganglion Cells in Goldfish

TSUGIHISA SASAKI, YUUSUKE NAKATANI, and KAZUHISA SUGIYAMA

ABSTRACT

Purpose: **Our aim was to examine the inhibitory effect of nilvadipine on voltage-gated calcium (Ca) channels in solitary ganglion cells.**

Methods: **Eyes were excised from goldfish. Ganglion cells were enzymatically dissociated from isolated retina. Whole-cell currents were recorded with the perforated-patch clamp technique.**

Results: **Depolarizing step pulses to more than −48 mV evoked a slowly inactivating inward Ca current. The current-voltage relation for the nilvadipine-sensitive current was bell-shaped, and the peak current reached a maximum at −8 mV in the presence and absence of nilvadipine. Nilvadipine block of voltage-gated Ca current was dose-dependent between 1 and 100 μM. The half-maximum inhibitory dose was 35 μM.**

Conclusions: **The inhibitory effect of orally administered nilvadipine on Ca channels had a mild influence in ganglion cells.**

INTRODUCTION

REDUCTION OF INTRAOCULAR PRESSURE is the first choice to treat primary open-angle glaucoma (POAG). Clearly, an excessive increase in intracellular calcium (Ca^{2+}) concentration can activate cytotoxic mechanisms associated with injury in various cell systems and organs.[1] Some studies have suggested that the favorable effect of organic Ca^{2+} antagonists on ischemic brain damage may result partly from their inhibitory action on the voltage-gated Ca^{2+} channels of the neurons.[2–4]

Nilvadipine, a dihydropyridine derivative, is an L-type Ca^{2+} channel blocker. It has selective and long-lasting effects on cerebral arteries, compared with other Ca^{2+} antagonists, such as nifedipine and diltiazem.[5] Nilvadipine is used predominantly as an antihypertensive agent and as a potent vasodilator for increasing cerebral blood flow circulation after a stroke. Its effectiveness in protecting the visual field and improving retrobulbar perfusion has been reported.[6] There is evidence for an effect of nilvadipine on voltage-gated Ca^{2+} channels in freshly isolated pyramidal neurons, which are known to be highly sensitive to ischemia.[7] Fish retinal ganglion cells and other neurons express multiple types of pharmacologically distinct, voltage-gated Ca^{2+} channels[8,9] involved in neuron excitability, intracellular Ca^{2+} regulation, and neurotransmitter release. However, the direct effect of nilvadipine on retinal ganglion cells is still unclear. Therefore, in this study, we used an amphotericin B-perforated patch recording technique to investigate the inhibitory effects of nil-

Department of Ophthalmology, Kanazawa University School of Medicine, Kanazawa, Japan.
The authors have no financial or material support from the manufacturer of any commercial product mentioned in this paper.

vadipine on voltage-gated Ca^{2+} channels in freshly isolated retinal ganglion cells under voltage-clamp conditions.

METHODS

The protocol was approved by the University Animal Care Committee, and the care of the animals was in accordance with guidelines for the Care and Use of Laboratory Animals, Kanazawa University School of Medicine (Kanazawa, Japan).

Dissociation and identification of the goldfish retinal ganglion cells and the liquid junction potential correction technique have been described previously.[10,11] Briefly, 8- to 10-cm dark-adapted goldfish were pithed under tricaine methasulfonate anesthesia (1% in solution bath), their enucleated eyes were hemisected, and the retina was separated from the retinal pigment epithelium. The isolated retina was incubated in well-oxygenated standard external solution (135 mM NaCl, 5 mM KCl, 2 mM $MgCl_2$, 2 mM $CaCl_2$, 10 mM N-2-hydroxyethylpiperazine-N'-2,4-ethanesulfonic acid [HEPES], 10 mM glucose, and 0.0003 mM tetrodotoxin [TTX; Sankyo Co., Tokyo, Japan], pH 7.4 adjusted with NaOH), containing 10 U/mL papain (Worthington; Lakewood, NJ) and 0.1 mg/mL cysteine (Sigma; St Louis, MO) at 28°C for 30 min. The ganglion cells were then dispersed mechanically with fire-polished glass pipettes. Dissociated cells were plated onto the coverslip of the recording chamber. Recordings were made at room temperature (19–22°C).

Dissociated cells were identified as ganglion cells by morphological features described previously[12] or by the presence of 1,1'-dioctadecyl-3,3,3',3'-tetramethylindocarbocyanine perchlorate (DiI; Invitrogen, Carlsbad, CA) transported retrogradely through the optic nerve. The electrophysiological recordings were made in the amphotericin B-perforated patch recording configuration under voltage-clamp conditions.[13]

To minimize contamination by voltage-dependent potassium and sodium currents, cells were superfused with a solution containing Cs, tetraethylammonium (TEA), and TTX. The experimental solution for Ca^{2+} current (I_{Ca}) recording (4 mM Ca^{2+} solution) was: 79 mM NaCl, 10 mM KCl, 1 mM $MgCl_2$, 4 mM $CaCl_2$, 10 mM CsCl, 25 mM TEA-Cl, 10 mM HEPES, 16 mM glucose, and 0.0003 mM TTX, pH 7.4 adjusted with NaOH. Pipettes were filled with a solution containing 120 mM CsOH, 30 mM TEA-Cl, 3 mM $CaCl_2$, 3 mM $MgCl_2$, 10 mM 1,2-bis(2 aminophenoxy) ethane-N,N,N',N',-tetraacetic acid (BAPTA), and 5 mM HEPES, pH 7.5 adjusted with methanesulfonic acid. The shanks of these pipettes were filled with this solution after addition of a 1:100 dilution of a stock solution of amphotericin B (0.5% wt/vol in dimethyl sulfoxide [DMSO]; Sigma). Nilvadipine (100 mM in DMSO; Astellas Pharma Inc, Tokyo, Japan), Nifedipine (10 mM in ethanol; Sigma) and ω-conotoxin GVIA (ω-CTX GVIA Nakalai Tesque, Kyoto, Japan) was diluted with experimental solution. The pipette resistance in the bath solution was approximately 7 MΩ when filled with pipette solution. The recording pipette was connected to a low-noise current-voltage converter (EPC-8; List-Medical, Darmstadt, Germany). The bath solution was connected to the Ag/AgCl bath electrode by a 1% agar bridge. Data were sampled at 10 kHz after passing through a low-pass filter with a cut-off frequency of 5 kHz. Stored data were analyzed offline on a personal computer (ibook; Apple Computer, Cupertino, CA). Stimulus generation, data acquisition, and plotting were controlled by the Pulse and Pulse-fit programs (List-Medical; Darmstadt). All currents were corrected for linear leak and capacitative currents using scaled currents elicited by depolarization or hyperpolarization from a holding potential (Vh). Perforated-patch access occurred usually in 5 min, and series resistance was compensated. The perforated-patch technique prevents the run-down of voltage-dependent calcium current and allows stable current recording for over 1 h. Solution was perfused by rapid superfusion with a U-tube system.[14]

RESULTS

The blocking effect of 30 μM of nilvadipine reached a plateau within 2 min and declined partially within 5 min after washout of nilvadipine (Fig. 1). To obtain steady-state inhibition of I_{Ca}, recordings were started 2 min after the start of drug application, except for ω-CTX GVIA application. To examine the effect of ω-CTX GVIA, I_{Ca} recordings were started 3 min after the start of drug application because the increase in blocking effect was more gradual.[8] Superfusion with nilvadipine (10 μM) caused decrease in the I_{Ca} amplitude, but only partial recovery was observed over a 5-min period following washout of the drug. Cells were held at a potential of −88 mV and then stepped in 10-mV increments from −88

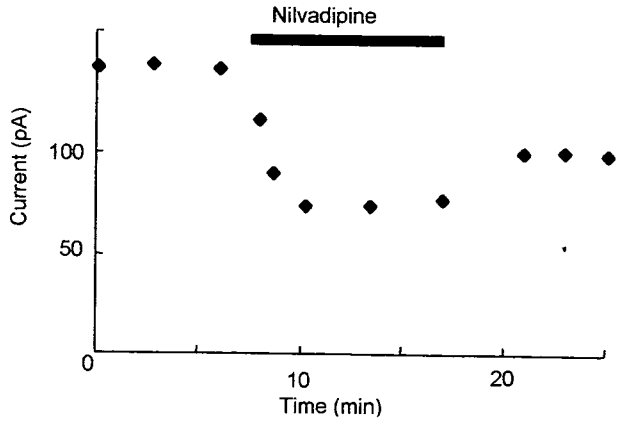

FIG. 1. Inhibition of calcium current (I_{Ca}) by nilvadipine. Time course of current block by 30 μM nilvadipine. Peak inward current was elicited at −8 mV and plotted against time. Full recovery from nilvadipine is not observed. Bar: period of nilvadipine application.

mV to +52 mV in the absence and presence of nilvadipine to study the current-voltage relations of I_{Ca}. When cells were held at −88 mV and a step pulse to −48 mV for 200 msec was applied, inward current started to flow without detectable delay and inactivated slowly (Fig. 2, inset). Current amplitude at the peak (peak current) and at the end of the command pulse (steady current) were measured and plotted against the step pulses (Fig. 2). At approximately −8 mV, the current reached a maximum. At more positive voltages than −8 mV, the current amplitude decreased gradually. For the steady current, the threshold voltage and the voltage at which the peak amplitude was recorded were nearly identical to those of the peak current. In the presence of nilvadipine, current amplitude was reduced at all voltages (Fig. 2, inset), but the threshold voltages and voltages at the amplitude of the peak and steady current did not change. At more positive voltages, the peak and steady current amplitude were reduced.

The inhibitory actions of nilvadipine on the peak I_{Ca} were normalized to I_{Ca} recorded without nilvadipine, and the pooled data were averaged and plotted against the nilvadipine concentration (Fig. 3). The lowest nilvadipine concentration giving a detectable effect was 1 μM. Further increases in the concentration of nilvadipine reduced I_{Ca} amplitude in a concentration-dependent manner. Data points were fitted by least square method to a Hill equation with a half-maximum inhibitory dose (IC_{50}) of approximately 35 μM. To determine which subtypes of Ca^{2+} channels were blocked by nilvadipine, the following experiments were performed. To avoid the contamination of low-voltage-activated (LVA) I_{Ca}, ganglion cells were voltage-clamped at a Vh of −48 mV (the potential at which LVA Ca^{2+} channels are inactivated).[7,15] The application of 1 μM ω-CTX GVIA inhibited the high-voltage-activated (HVA) I_{Ca} by 72.3% ± 7.1% (n = 4). After exposure to 1 μM ω-CTX GVIA, exposure to 1 μM nifedipine inhibited HVA I_{Ca} by 92.0% ± 8.7% (n = 4). After complete blockage of L- and N-type current by 2 pharmacological agents (1 μM nifedipine and 1 μM ω-CTX GVIA), 1 μM nilvadipine did not block the residual currents (n = 4), which include P/Q- and R-type I_{Ca} (Fig. 4). These results suggest that low-concentration nilvadip-

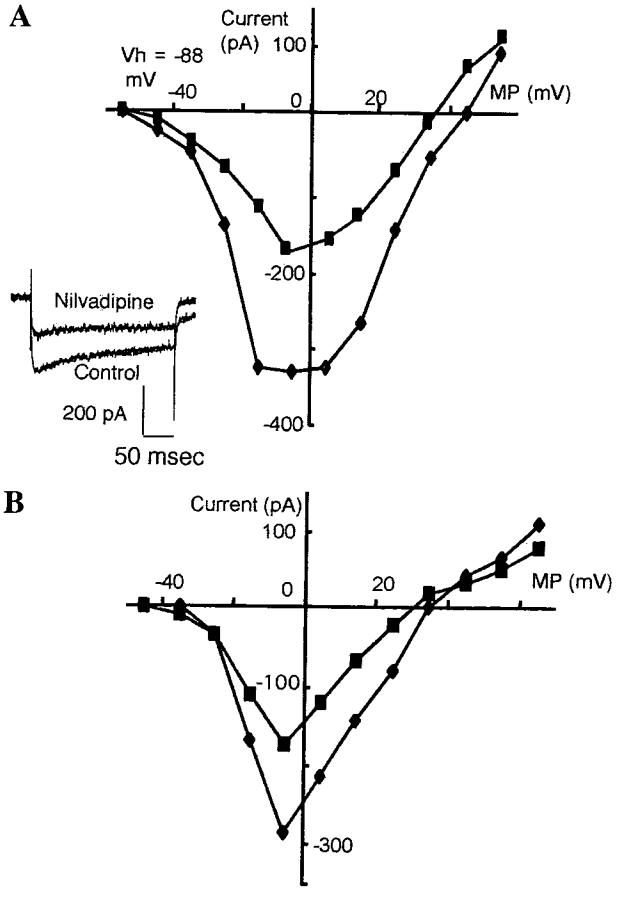

FIG. 2. The perforated-patch clamp technique was used to monitor current-voltage (I-V) relations for I_{Ca} in isolated goldfish ganglion cells in control solution (◆) and in control solution with 10 μM nilvadipine (■). I_{Ca} was recorded at a holding potential (Vh) of −88 mV, which was then stepped up in 10-mV increments from −88 to +52 mV. (**A**) I-V relation recorded at the peak current amplitude. (**B**) I-V relation recorded at the end of the command pulse. The inset shows representative current traces recorded at +2 mV in the control and in 10-μM nilvadipine solutions.

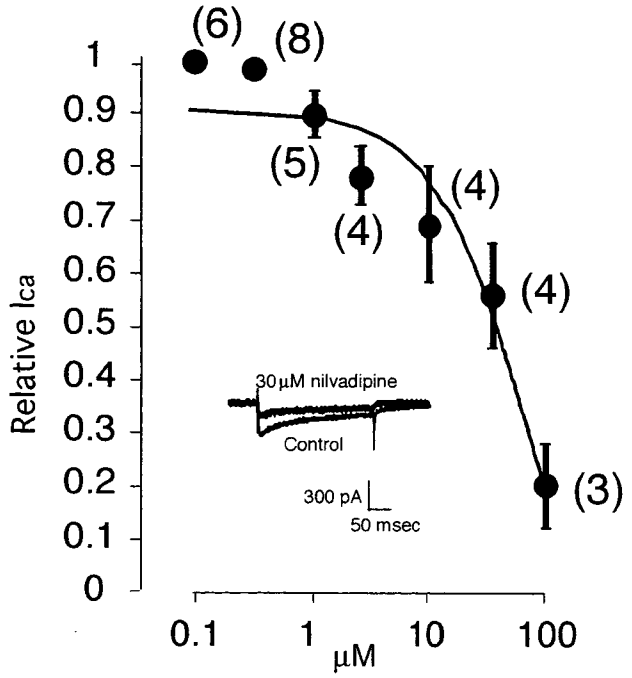

FIG. 3. Dose-response relations for nilvadipine. Cells were depolarized to −8 mV for 200 msec from a Vh of −88 mV. The response of I_{Ca} to a given nilvadipine concentration is expressed as the value of I_{Ca} relative to that evoked without nilvadipine. The inset provides representative current traces recorded at −8 mV in the control and 30 μM nilvadipine solutions. Each point is the average value from a group of cells (number of cells in parentheses), and vertical lines show standard deviation. Data points were fitted by least square method to a Hill equation.

ine blocked the L-type Ca^{2+} channels selectively in goldfish ganglion cells. High-dose nilvadipine (> 10 μM) blocked other types of I_{Ca}.

DISCUSSION

This study shows that nilvadipine at more than 1 μM inhibits voltage-gated calcium channels in acutely dissociated goldfish retinal ganglion cells.

Nilvadipine (100 μM) reduced I_{Ca} amplitude by 81%, whereas low-dose nilvadipine (< 1 μM) reduced I_{Ca} amplitude, at most, 10%. ω-CTX GVIA, an N-type specific blocker, suppressed 72% of HVA I_{Ca}. These results indicate that N- and L-type I_{Ca} constitute at least 72% and 20% of total I_{Ca} in ganglion cells, respectively, and that a low dose of nilvadipine blocked L-type Ca^{2+} channels. Cyprinid retinal ganglion cells possess as many as three types of I_{Ca}. One, which is responsible for at least three fourths of the total I_{Ca}, is blocked by ω-CTX GVIA.[8] This finding coincides with our results. It is thought that a large portion of I_{Ca} blockage by high-dose nilvadipine (> 10 μM) and nifedipine is a result of nonspecific effects on L- and N-type Ca channels.[16–19]

The IC_{50} of nilvadipine for inhibition of I_{Ca} is 35 μM. The reported concentration in rat cerebrum after intravenous or oral application of nilvadipine was 1.1–2.6 μM.[20] The L-type Ca channel current constitutes one fifth of the total I_{Ca} in ganglion cells. Therefore, orally administered nilvadipine might show a mild suppressive effect on voltage-gated calcium channels. The effect of nilvadipine on ganglion cells may be mild and, therefore, provide only mild protection from progressive deterioration of the visual field in POAG patients. On the other hand, nimodipine and nicardipine do protect the brain against ischemic damage.[21] The ganglion cells in this study had no distal dendrites. Nilvadipine might affect other neurons and glia, as these cells have L-type Ca^{2+} channels.[22,23] New drugs that prevent ischemia-induced neuronal damage by inhibiting N- and L-type Ca^{2+} channels should be investigated.

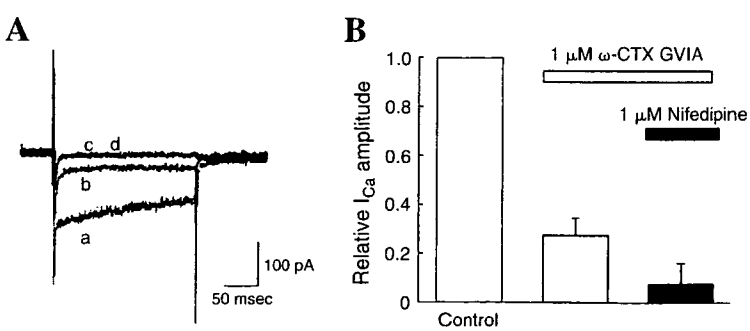

FIG. 4. Effects of nilvadipine on the ω-conotoxin GVIA (ω-CTX GVIA) and nifedipine-insensitive high-voltage-activated (HVA) I_{Ca} components. HVA I_{Ca} was evoked by a depolarizing step from Vh of −48 mV to +2 mV. (**A**) Superimposed current traces in control conditions and in the presence of these Ca^{2+} antagonists applied cumulatively. Current traces (a–d) were obtained in a: control solution, or in the presence of b: ω-CTX GVIA, c: ω-CTX GVIA + nifedipine, or d: ω-CTX GVIA + nifedipine + nilvadipine. All concentrations of the antagonists were 1 μM. Trace d is drawn faintly for clarity. (**B**) The residual HVA I_{Ca} after application of various Ca^{2+} antagonists. The amplitude of I_{Ca} was measured at the peak. Each point is the average value from a group of cells (n = 4) and vertical lines show standard deviations. Bar: application of Ca^{2+} antagonists.

CONCLUSION

The inhibitory effect of orally administered nilvadipine on Ca channels had a mild influence in ganglion cells.

ACKNOWLEDGMENTS

This work was supported by Grants-in-Aid for Scientific Research from the Ministry of Education, Science, and Culture to T. Sasaki (No. 16591741) and to Y. Nakatani (No. 16922200, No. 17925041). We are grateful to Dr. Makoto Kaneda for expert advice and useful discussions throughout this study.

REFERENCES

1. Choi, D.W. Calcium-mediated neurotoxicity: Relationship to specific channel types and role in ischemic damage. *Trends Neurosci.* 11:465–469, 1988.
2. Alps, B.J., Calder, C., Hass, W.K., et al. Comparative protective effects of nicardipine, flunarizine, lidoflazine, and nimodipine against ischaemic injury in the hippocampus of the Mongolian gerbil. *Br. J. Pharmacol.* 93:877–883, 1988.
3. Beck, T., Nuglisch, J., Sauer, D., et al. Effects of flunarizine on postischemic blood flow, energy metabolism, and neuronal damage in the rat brain. *Eur. J. Pharmacol.* 158:271–274, 1988.
4. Kawamura, S., Yasui, N., Shirasawa, M., et al. Effects of a Ca^{2+} entry blocker (nilvadipine) on acute focal cerebral ischemia in rats. *Exp. Brain Res.* 83:434–438, 1991.
5. Tokuma, Y., Fujiwara, T., and Noguchi, H. Absorption, distribution, and excretion of nilvadipine, a new dihydropyridine calcium antagonist, in rats and dogs. *Xenobiotica* 17:1341–1349, 1987.
6. Harris, A., Evans, D.W., Cantor, L.B., et al. Hemodynamic and visual function effects of oral nifedipine in patients with normal-tension glaucoma. *Am. J. Ophthalmol.* 124:296–302, 1997.
7. Ishibashi, H., Murai, Y. and Akaike, N. Effect of nilvadipine on the voltage-dependent Ca^{2+} channels in rat hippocampal CA1 pyramidal neurons. *Brain Res.* 813:121–127, 1998.
8. Bindokas, V.P., and Ishida, A.T. Conotoxin-sensitive and conotoxin-resistant Ca^{2+} currents in fish retinal ganglion cells. *J. Neurobiol.* 29:429–444, 1996.
9. Randall, A., and Tsien, R.W. Pharmacological dissection of multiple types of Ca^{2+} channel currents in rat cerebellar granule neurons. *J. Neurosci.* 15:2995–3012, 1995.
10. Kaneko, A., and Tachibana, M. Effects of gamma-aminobutyric acid on isolated cone photoreceptors of the turtle retina. *J. Physiol.* 373:443–461, 1986.
11. Tabata, T., and Ishida, A.T. Transient and sustained depolarization of retinal ganglion cells by Ih. *J. Neurophysiol.* 75:1932–1943, 1996.
12. Ishida, A.T., and Cohen, B.N. GABA-activated whole-cell currents in isolated retinal ganglion cells. *J. Neurophysiol.* 60:381–396, 1988.
13. Horn, R., and Marty, A. Muscarine activation of ionic currents measured by a new whole-cell recording method. *J. Gen. Physiol.* 92:145–159, 1988.
14. Suzuki, S., Tachibana, M., and Kaneko, A. Effects of glycine and GABA on isolated bipolar cells of the mouse retina. *J. Physiol.* 421:645–662, 1990.
15. Murai, Y., Uneyama, H., Ishibashi, H., et al. Preferential inhibition of L- and N-type calcium channels in the rat hippocampal neurons by cilnidipine. *Brain Res.* 31:6–10, 2000.
16. Ozawa, Y., Hayashi, K., Nagahama, T., et al. Effect of T-type selective calcium antagonist on renal microcirculation: Studies in the isolated perfused hydronephrotic kidney. *Hypertension* 38:343–347, 2001.
17. Furukawa, T., Yamakawa, T., Midera, T., et al. Selectivities of dihydropyridine derivatives in blocking Ca^{2+} channel subtypes expressed in Xenopus oocytes. *J. Pharmacol. Exp. Ther.* 291:464–473, 1999.
18. Jones, S.W., and Jacobs, L.S. Dihydropyridine actions on calcium currents of frog sympathetic neurons. *J. Neurosci.* 10:2261–2267, 1990.
19. Kaneda, M., and Kaneko, A. Voltage-gated calcium currents in isolated retinal ganglion cells of the cat. *Jpn. J. Physiol.* 41:35–48, 1991.
20. Takakura, S., Sogabe, K., Satoh, H., et al. Nilvadipine as a neuroprotective calcium entry blocker in a rat model of global cerebral ischemia. A comparative study with nicardipine hydrochloride. *Neurosci. Lett.* 20:199–202, 1992.
21. Izumiya, K., and Kogure, K. Prevention of delayed neuronal death in gerbil hippocampus by ion channel blockers. *Stroke* 19:1003–1007, 1988.
22. Kaneko, A., Suzuki, S., Pinto, L.H., et al. Membrane currents and pharmacology of retinal bipolar cells: A comparative study on goldfish and mouse. *Comp. Biochem. Physiol. C.* 98:115–127, 1991.
23. Puro, D.G., Hwang, J.J., Kwon, O.J., et al. Characterization of an L-type calcium channel expressed by human retinal Muller (glial) cells. *Brain Res. Mol. Brain Res.* 37:41–48, 1996.

Received: December 30, 2005
Accepted: July 14, 2006

Reprint Requests: *Tsugihisa Sasaki*
Department of Ophthalmology
Kanazawa University School of Medicine
Kanazawa, Ishikawa, 920-8641
Japan

E-mail: sasatsug@w5.dion.ne.jp

Available online at www.sciencedirect.com
ScienceDirect
Experimental Eye Research 84 (2007) 1039–1046
EXPERIMENTAL EYE RESEARCH
www.elsevier.com/locate/yexer

Vasodilatory mechanism of levobunolol on vascular smooth muscle cells

Yaru Dong [a,c], Hitoshi Ishikawa [b], Yazhen Wu [c], Takeshi Yoshitomi [a,*]

[a] Department of Ophthalmology, Akita University School of Medicine, 1-1-1 Hondo, Akita, Akita 010-8543, Japan
[b] Department of Orthoptics and Visual Sciences, School of Allied Health, Kitasato University, Kanagawa 228-8555, Japan
[c] Department of Ophthalmology, The Second Hospital of Jilin University, Jilin 130042, P.R. China

Received 14 August 2006; accepted in revised form 8 January 2007
Available online 27 January 2007

Abstract

Topical application of levobunolol hydrochloride, a β-adrenergic antagonist used for treatment of glaucoma, is reported to increase ocular blood flow. We studied the mechanism of levobunolol-induced vasodilation in arterial smooth muscle. The effects of levobunolol or other agents on isolated, pre-contracted rabbit ciliary artery were investigated using an isometric tension recording method. The effects of the same agents on intracellular free calcium ($[Ca^{2+}]_i$) in cultured human aortic smooth muscle cells were also studied by fluorophotometry. Levobunolol relaxed ciliary artery rings that were pre-contracted with either high-K solution, 1 μM histamine, 10 μM phenylephrine, or 100 nM endothelin-1. The relaxation induced by levobunolol was concentration-dependent over the range of 10 μM to 0.3 mM. Inhibition of endothelial nitric oxide synthase or denudation of the endothelium did not affect this relaxation. Histamine-induced contractions were inhibited by the histamine H_1 antagonist pyrilamine. Radioligand binding experiments showed that levobunolol did not bind to the H_1 receptor. Further, histamine induced transient contraction in Ca^{2+}-free solution, and levobunolol inhibited this contraction by 74.6 ± 11.0%. In cultured smooth muscle cells in the presence of extracellular Ca^{2+}, levobunolol significantly inhibited the histamine-induced elevation of $[Ca^{2+}]_i$. However, it did not inhibit the increase of $[Ca^{2+}]_i$ in histamine-stimulated cells incubated in Ca^{2+}-free solution. These results indicate that levobunolol may relax rabbit ciliary artery by two different mechanisms. First, the relaxation could be due to the blockade of Ca^{2+} entry through non-voltage-dependent Ca^{2+} channels. Second, levobunolol may change the Ca^{2+} sensitivity of vascular smooth muscle cells.

Keywords: Ca^{2+} channel; Ca^{2+} sensitivity; fura-2; levobunolol; relaxation; vascular smooth muscle

1. Introduction

Though it is generally accepted that increased intraocular pressure (IOP) is a major risk factor in glaucoma, vascular perfusion is also considered to be important in the pathogenesis of optic nerve damage and visual field loss, especially in patients with normal tension glaucoma (Collignon-Brach, 1994; Drance, 1998; Flammer, 1994). Therefore, a better understanding of the effect of antiglaucoma agents on ocular circulation is important for optimizing their clinical use. We have reported that timolol (Hayashi-Morimoto et al., 1999), betaxolol (Hayashi-Morimoto et al., 1999), pilocarpine (Yoshitomi et al., 2000), unoprostone isopropyl (Yoshitomi et al., 2004), latanoprost (Ishikawa et al., 2002) and nipradilol (Yoshitomi et al., 2002) induced relaxation of the isolated rabbit ciliary artery. Each of these drugs acts through different mechanisms. For example, betaxolol (Hayashi-Morimoto et al., 1999) and nipradilol (Yoshitomi et al., 2002), both β-adrenergic antagonists, relaxed rabbit ciliary artery. Betaxolol can inhibit voltage depended calcium (Ca^{2+}) channel in this tissue (Hayashi-Morimoto et al., 1999) which also were seen in other tissue such as guinea-pig mesenteric artery and portal

* Corresponding author. Tel.: +81 18 884 6164; fax: +81 18 836 2621.
E-mail address: yoshitom@med.akita-u.ac.jp (T. Yoshitomi).

0014-4835/$ - see front matter © 2007 Elsevier Ltd. All rights reserved.
doi:10.1016/j.exer.2007.01.010

vein smooth muscle cells (Setoguchi et al., 1995). On the other hand, nipradilol relaxed rabbit ciliary artery by inducing nitric oxide (NO) production and blocking α-adrenergic receptor (Yoshitomi et al., 2002). We have reported that isoproterenol, a β-adrenergic agonist, has no effect on mechanical properties of rabbit ciliary artery (Hayashi-Morimoto et al., 1999). So, vasodilatory action of these β-adrenergic antagonists seems to be unrelated to the β-adrenergic receptor and have different mechanism in each agent. Various antiglaucoma agents including β-adrenergic antagonists also increase ocular blood flow in vivo (Arend et al., 1998; Georgopoulos et al., 2002; Grunwald, 1990; Kimura et al., 2005; Shaikh and Mars, 2001), but this effect seem not to be generated by decreasing IOP. Chiou et al. (1990) have reported that D-timolol which is less potent than L-timolol to lower IOP, is more potent than L-timolol to improve blood flow in retina and choroid of rabbit. There are also other reports that betaxolol may increase significantly ciliary body blood flow, choroidal blood flow, and retinal blood flow in rabbits' eyes in vivo (Sato et al., 2001). Levobunolol, a non-selective β-adrenergic antagonist, is widely used in antiglaucoma treatment. A number of clinical trials have suggested that levobunolol also can improve ocular circulation (Arend et al., 1998; Bosem et al., 1992; Morsman et al., 1995; Ogasawara et al., 1999). Morsman et al. (1995) reported that pulsatile ocular blood flow increased by 22% after 1 week's administration of levobunolol. Arend et al. (1998) indicated that levobunolol produced a decrease in arteriovenous passage time of approximately 25%, and it increased macular capillary blood velocity by approximately 20%. Concerning the vasodilatory mechanism of levobunolol, Wu et al. (2004), using a spectrofluorometry method, indicated that levobunolol inhibits the intracellular Ca^{2+} increases by blocking the L-type voltage-dependent Ca^{2+} channel. However, the underlying mechanisms of its effects on ocular circulation are not yet clear.

In an attempt to clarify the vasodilatory mechanism of levobunolol, we have investigated the effect of this drug using an isometric tension recording method on isolated rabbit ciliary artery. Additionally, we used fluorescence photometry to measure the effect of levobunolol on intracellular Ca^{2+} levels in cultured human aortic artery smooth muscle cells.

2. Materials and methods

2.1. Isometric tension recording method in isolated ciliary arteries

All animals were treated in accordance with the ARVO Statement for the Use of Animals in Ophthalmic and Vision Research and in approval by Animal Experiment Committee of Akita University. Male albino rabbits weighing 2–3 kg were killed with an overdose of intravenous pentobarbital sodium (Abbott, North Chicago, IL, USA). The eyes were immediately enucleated, ensuring that a maximum length of optic nerve was removed, and then placed in oxygenated Krebs solution of the following composition (mM): NaCl 94.8, KCl 4.7, $MgSO_4 \cdot 7H_2O$ 1.2, $CaCl_2$ 2.5, KH_2PO_4 1.2, $NaHCO_3$ 25.0, glucose 11.7 and aerated with 95% O_2 and 5% CO_2. With the aid of a dissecting microscope, the ciliary artery and surrounding connective tissue were carefully isolated from the optic nerve. Vascular ring segments (150–300 μm in diameter, 1–2 mm in length) were cut from the distal section of the ciliary artery and mounted in a chamber of the double Myograph System® (JP Trading, Denmark) with Krebs solution. After a process of the temperature rose to 37 °C in the chamber, the vessels were stretched to each optimal lumen diameter for active tension development, i.e. normalization. Then the vessels were equilibrated for 30 min. The Myograph System® allowed direct determination of vessel isometric tension while the internal circumference was controlled. Detailed methods for isometric tension recordings by the Myograph System® have been described by Mulvany and Halpern (1976, 1977).

After the equilibration period, the amplitudes of the contractions were evoked by the high-K solution and were measured at 20-min intervals to establish preparation viability and stability. High-K solutions were prepared by replacing NaCl with isotonic, equimolar KCl to give a final K^+ concentration of 100.7 mM. Cholinergic agonists, acting on receptors in the endothelium, were applied at 20-min intervals of the contraction and induce relaxation of vascular smooth muscle (Keef and Bowen, 1989). Thus, we tested the susceptibility of contracted ciliary arteries to cholinergic relaxation with 1 μM carbachol. All preparations entirely underwent the contraction and relaxation described above, before the separate experiments. In certain experiments, the vascular rings in baseline tone were incubated with inhibitor 30 min before the separate experiment. In other experiments, we gently denuded the endothelium by rubbing the inside of the vascular ring with a scalp hair before the normalization.

Additionally, the ability of levobunolol to relax ciliary artery rings pre-contracted with other agents, including histamine, phenylephrine, and endothelin-1, and in Ca^{2+}-free media was also determined. Generally, the pre-contraction was maintained for 20 min, then levobunolol was applied every 10 min in a cumulative manner. The Ca^{2+}-free solutions were prepared by replacing $CaCl_2$ with isotonic, equimolar $MgCl_2$ and adding 1 mM EGTA, a chelating agent for Ca^{2+} in the presence of magnesium. The ability of the H_1 histamine antagonist pyrilamine, the H_2 histamine antagonist cimetidine, and the L-type voltage-dependent Ca^{2+} channel blocker diltiazem to induce relaxation of contracted ciliary artery rings was also tested.

2.2. Smooth muscle cell cultures

Human aortic smooth muscle cells at passage 3 were purchased from Cambrex (Walkersville, MD, USA). The cells were grown in the culture medium (SmGM-2, Sanko Junyaku Co. Ltd., Tokyo, Japan) in 5% CO_2-containing air at 37 °C. The culture medium was exchanged every 48 h until a subconfluent growth stage was obtained. The cells were detached by exposure for approximately 3 min to 0.025% trypsin in

a Ca^{2+}- and Mg^{2+}-free solution containing 0.01% EDTA. The detached cells were diluted in the culture medium, and then reseeded with a cell density of approximately 2500 cells/cm^2 on coverslips (9 × 9 mm) coated with fibronectin (Biomedical technologies, Stoughton, MA, USA). The cells were maintained in culture for 1–4 days before use.

2.3. Intracellular Ca^{2+} determination by fluorescence photometry

To determine intracellular Ca^{2+} levels, cultured smooth muscle cells were loaded with 10 μM fura-2 acetoxymethyl ester at 37 °C for 30 min in HEPES-buffered saline (HBS). HBS containing 5 mM $CaCl_2$ instead of 1 mM $CaCl_2$ was used as a standard bath solution. Thereafter, cells were rinsed several times with HBS to remove extracellular fura-2 and used for experiments within 3 h. Changes of intracellular free calcium concentration $[Ca^{2+}]_i$ in individual cells were measured using an Aquacosmos System (Hamamatsu Photonics kk, Shizuoka, Japan) equipped with a Nikon epifluorescence microscope (TE2000-U; Nikon, Tokyo, Japan) and band-pass filters for wavelengths of 340 and 380 nm. After correction for the individual background fluorescence, the ratio of the fluorescence at both excitation wavelengths (F_{340}/F_{380}) was monitored simultaneously to determine the $[Ca^{2+}]_i$. In the present experiments, the amplitude of $[Ca^{2+}]_i$ induced by the first application of 1 μM histamine was defined as 100%. Values were expressed as percents of $[Ca^{2+}]_i$ in the first application.

2.4. Radioligand binding assays to human recombinant receptors

Cloned human recombinant histamine receptors were commercially obtained (H_1: Cat. No. ES-390-M; H_2: Cat. No. ES-391-M, Euroscreen SA, Gosselies, Belgium). Radioligand binding studies to H_1 and H_2 receptors were carried out with [^{3}H]pyrilamine (Cat. No. TRK608; GE Healthcare Bio-Sciences) and [^{3}H]tiotidine (Cat. No. NET688; PerkinElmer Life & Analytical Sciences), respectively. Detailed methods for radioligand binding assays have been described by Nguyen et al. (2001) with minor modifications. Affinity of the competing ligand was expressed as the percent inhibition of radioligand binding, $[(B - N)/(B_0 - N)] \times 100$, where B is the total bound radioactivity in the presence of competing ligand, B_0 is the mean total bound radioactivity in the absence of competing ligand, and N is the mean non-specifically bound radioactivity.

2.5. Drugs

The following drugs and chemicals were used: carbachol hydrochloride, histamine, ethylene glycol-bis (2-aminoethylether)-*N,N,N,N*-tetraacetic acid (EGTA), endothelin-1, cimetidine, pyrilamine (all from Sigma Chemical Co., St. Louis, USA), phenylephrine hydrochloride, N^G-nitro-L-arginine methylester (L-NAME), diltiazem (all from Wako Chemical, Osaka, Japan), and levobunolol hydrochloride (Kaken Pharm, Tokyo, Japan). Concentrations were expressed as final molar concentrations in the organ chambers.

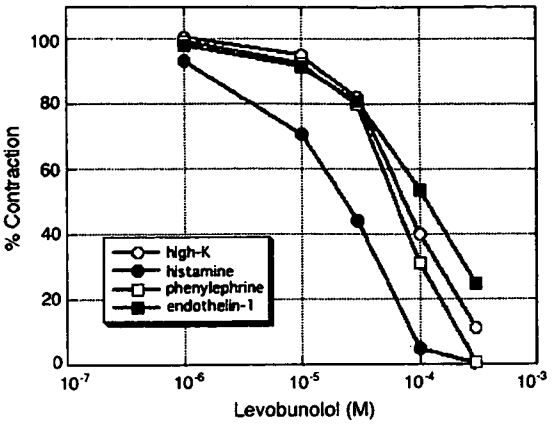

Fig. 1. Levobunolol-induced relaxation of pre-contracted rabbit ciliary arteries. Levobunolol induced concentration-dependent relaxation in the arterial rings that were pre-contracted with high-K solution ($n = 8$), 1 μM histamine ($n = 8$), 10 μM phenylephrine ($n = 11$) or 100 nM endothelin-1 ($n = 10$). The amplitude of contraction induced by High-K solution was defined as 100%.

2.6. Statistical analysis

Results were expressed as means ± S.D. with n representing the number of vessels or cells studied. The concentrations of drugs causing 50% of the maximum relaxation (EC_{50}) were expressed as the log M concentration. Statistical differences between values were determined by the unpaired two-tailed Student's t-test. Differences between the concentration–response curves were analyzed by two-way analysis of variance (ANOVA). $P < 0.05$ was considered statistically significant.

3. Results

Stimulation with 1 μM histamine, 10 μM phenylephrine or 100 nM endothelin-1 elicited nearly the same level of contraction in this preparation as that induced by the high-K solution. Levobunolol caused a concentration-dependent relaxation of the vascular rings that were pre-contracted by each of these agents (Fig. 1). The minimum concentration of levobunolol that induced relaxation was 10 μM. Contractions induced by histamine, phenylephrine, high-K solution, and endothelin-1 were relaxed by 99.7%, 99.6%, 88.9% and 75.1%, respectively

Table 1
Inhibitory effect of levobunolol on radioligand binding to histamine receptors

Receptor ([^{3}H-ligand)	Inhibition (%)	
	Levobunolol	Receptor-specific ligand
Histamine H_1 ([^{3}H]pyrilamine)	0.0	99.8 (pyrilamine)
Histamine H_2 ([^{3}H]tiotidine)	28.8	99.2 (cimetidine)

Competing ligand concentration: 10 μM.

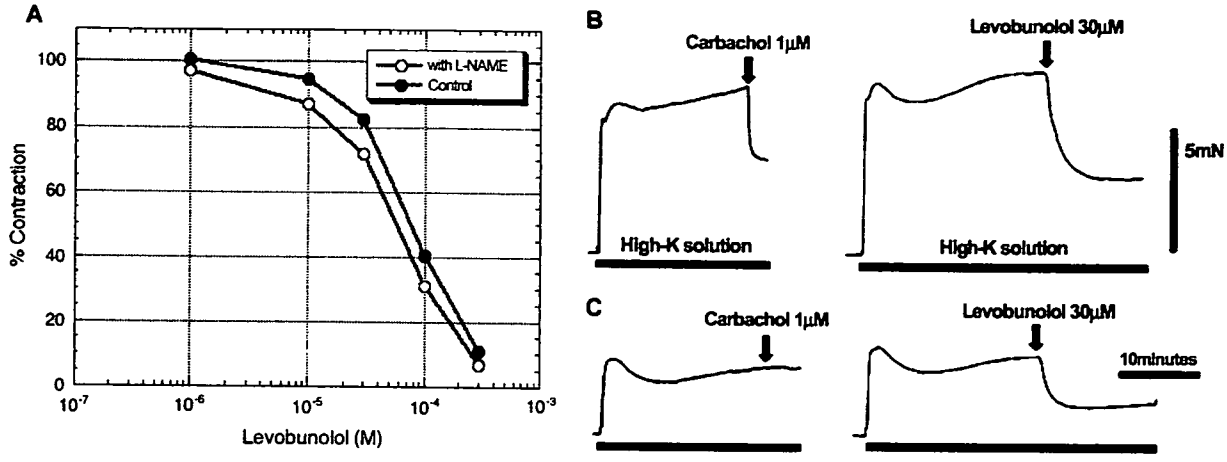

Fig. 2. Effects of L-NAME or denudation of endothelium on levobunolol-induced relaxation of rabbit ciliary arteries. (A) L-NAME (300 μM; $n = 6$) did not significantly alter ($P > 0.05$) the concentration-response curve for relaxation of high-K contracted ciliary arteries. The amplitude of contraction induced by high-K solution was defined as 100%. (B) Both carbachol (1 μM) and levobunolol (30 μM) induced relaxation in high-K pre-contracted ciliary artery. (C) In ciliary arteries denuded of the endothelium, carbachol (1 μM) did not induce relaxation. Denudation did not affect the response to levobunolol. The vertical bar with 5mN represents the actual isometric tension of rabbit ciliary arteries in myograph system.

with 30 mM levobunolol. Levobunolol was more effective in relaxing histamine-induced contractions ($EC_{50} = 20.7 \pm 16.3$ μM, $n = 8$) compared to phenylephrine, high-K or endothelin-1 induced contractions ($EC_{50} = 60.8 \pm 15.3$ μM, $n = 11$; $EC_{50} = 80.3 \pm 12.6$ μM, $n = 8$; $EC_{50} = 106.7 \pm 23.2$ μM, $n = 10$, respectively; Fig. 1).

Cimetidine (100 μM), a histamine H_2 receptor antagonist, did not relax the ciliary arteries pre-contracted with histamine (data not shown). On the other hand, 10 nM pyrilamine, a histamine H_1 antagonist, completely relaxed the histamine-contracted ciliary arteries (data not shown). These results indicated that the H_1 receptor was responsible for histamine induced vascular contraction. To determine if the relaxation effect of levobunolol could be mediated through either of the histamine receptors, we measured the displacement of receptor-specific radiolabeled ligands by levobunolol. Levobunolol had no effect on [^{3}H]pyrilamine binding to the histamine H_1 receptor (Table 1), but it did inhibit 28.8% of ^{3}H-tiotidine binding to the histamine H_2 receptor.

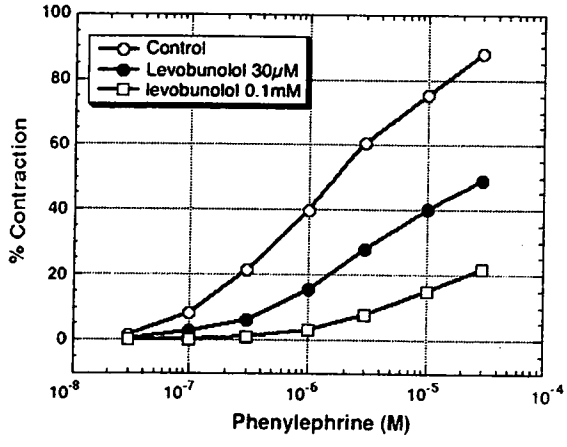

Fig. 3. Effects of levobunolol on phenylephrine concentration-dependent contractions of rabbit ciliary arteries. Levobunolol at 30 μM ($n = 10$) and at 100 μM ($n = 10$) significantly reduced the contractile response to phenylephrine ($P < 0.05$, $n = 14$). The amplitude of contraction induced by high-K solution was defined as 100%.

Pretreatment with 300 μM L-NAME did not changed the levobunolol induced concentration-dependent relaxation of the ciliary artery (Fig. 2A). Denudation of the vascular endothelium also had no effect on the 30 μM levobunolol-induced relaxation although it completely abolished the carbachol-induced relaxation (Fig. 2B,C).

Phenylephrine provoked concentration-dependent contractions in this preparation (Fig. 3). Pretreatment of levobunolol depressed the contractions. However, it did not shift the phenylephrine concentration-response curve to the right.

We compared the relaxing effect of 0.1 mM levobunolol and 1 μM diltiazem in the same preparations that were pre-contracted with either high-K solution or 1 μM histamine (Fig. 4). These concentrations were chosen because they produced approximately 50% relaxation in the high-K pre-contracted arterial rings. Levobunolol induced 59.2 ± 3.6% relaxation of the high-K pre-contracted preparations ($n = 6$), and 89.7 ± 4.2% of the 1 μM histamine ($n = 6$) pre-contracted preparations (Fig. 4A,B). In contrast, diltiazem induced 63.4 ± 7.6% relaxation of the high-K pre-contracted preparations ($n = 6$), but only 40.0 ± 7.2% of the 1 μM histamine ($n = 6$) pre-contracted preparations (Fig. 4C,D).

In Ca^{2+}-free solutions, 1 μM histamine induced a transient contraction of the ciliary artery (Fig. 5). Pretreatment of levobunolol (0.1 mM) markedly inhibited this contraction by 74.6 ± 11.0% (Fig. 5A,B). After a 30 min washout of the levobunolol, the transient contractions were almost completely restored.

In Ca^{2+}-containing Krebs solution, $[Ca^{2+}]_i$ of cultured human aortic smooth muscle cells was elevated by 1 μM

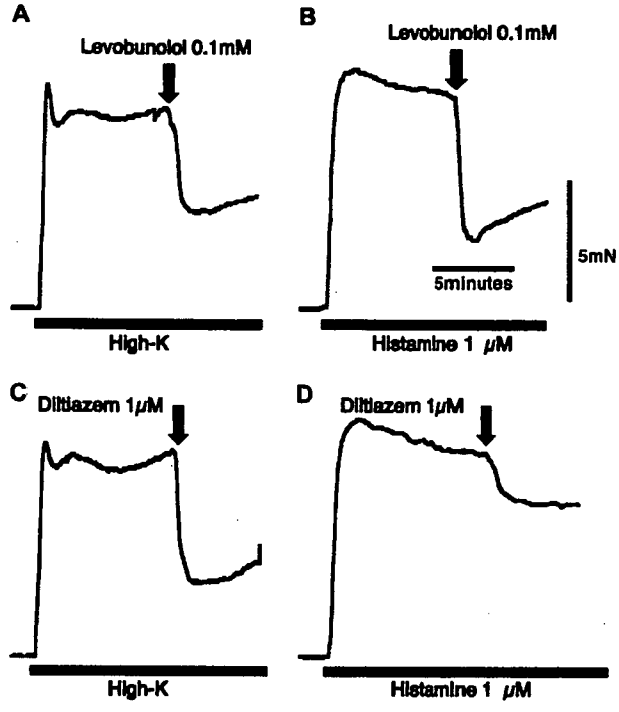

Fig. 4. Effects of levobunolol and diltiazem on high-K or histamine pre-contracted rabbit ciliary arteries. (A) Levobunolol (0.1 mM) induced less relaxation in preparations pre-contracted with high-K ($n = 6$) than with (B) histamine (1 μM, $n = 6$). (C) On the other hand, diltiazem (1 μM) induced a greater relaxation in high-K contracted arteries ($n = 6$) compared to (D) histamine (1 μM) contracted arteries ($n = 6$). The vertical bar with 5mN represents the actual isometric tension of rabbit ciliary arteries in myograph system.

histamine. After a 7 min washout, the amplitude of the $[Ca^{2+}]_i$ response to a second application of 1 μM histamine decreased by 27.6 ± 6.9% (Fig. 6A). To determine the effect of levobunolol on the histamine induced $[Ca^{2+}]_i$ increase, 3 μM levobunolol was added to the incubation medium just after washing out the first application of histamine. The amplitude of the $[Ca^{2+}]_i$ due to the second application of histamine in the presence of 3 μM levobunolol was decreased 45.9 ± 18.9%, a significantly greater decrease than the control (Fig. 6B, Table 2); whereas in Ca^{2+}-free solution, 3 μM levobunolol had no effect on $[Ca^{2+}]_i$ increase with 1 μM histamine (Fig. 6C,D, Table 2). Pyrilamine (10 nM) completely inhibited the elevation of $[Ca^{2+}]_i$ by 1 μM histamine in both the Ca^{2+}-containing Krebs solution and in the Ca^{2+}-free solution (Fig. 6E,F).

4. Discussion

The present studies demonstrated that levobunolol, a β-adrenergic antagonist, relaxed rabbit ciliary arteries that were pre-contracted with high-K solution, histamine, phenylephrine, or endothelin-1. These agents contract vascular smooth muscle by variety of mechanisms. The high-K solution induces contractions that depend on the passage of extracellular Ca^{2+} through voltage-dependent Ca^{2+} channels (Gustafsson, 1993). Histamine provokes contractions using Ca^{2+} that enters through voltage-dependent and receptor-dependent Ca^{2+} channels, as well as from intracellular Ca^{2+} stores (Laporte and Laher, 1997). Phenylephrine induces contraction through activation of α_1-adrenergic receptors that open voltage-dependent Ca^{2+} channels and induce Ca^{2+} release from intracellular Ca^{2+} stores (Eckert et al., 2000). Endothelin-1 is one of the most potent vasoconstrictors (Highsmith et al., 1989; Murakawa et al., 1990). When it binds to either G-protein-linked endothelin

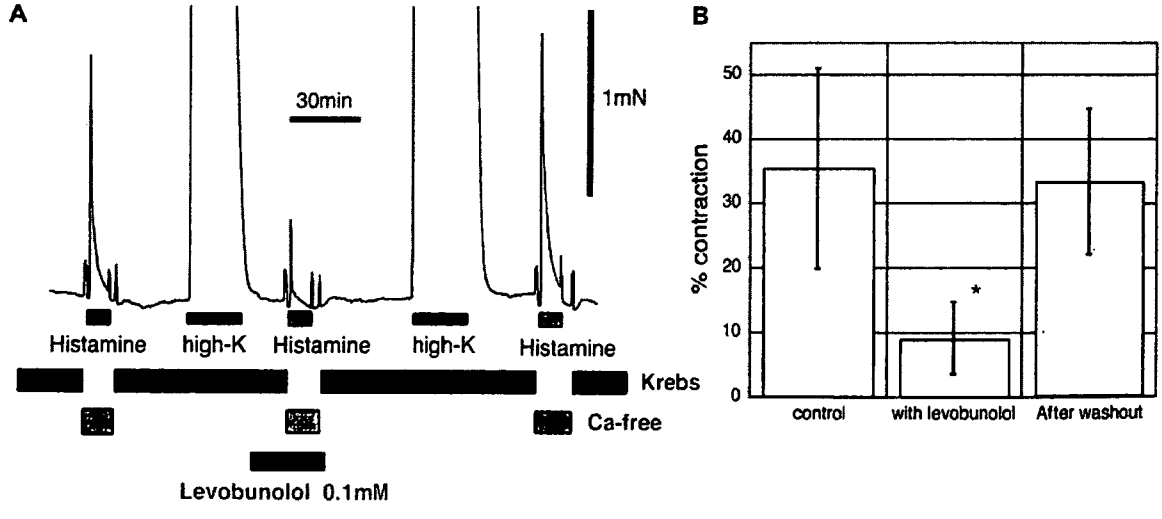

Fig. 5. Effects of levobunolol on histamine-induced transient contraction of rabbit ciliary arteries in Ca^{2+}-free solution. (A) Histamine (1 μM) was applied 6 min after incubation in Ca^{2+}-free solution. This was followed by high-K solution-induced contraction. Afterwards, the preparation was washed out with Krebs solution containing levobunolol (0.1 mM). (B) The amplitude of histamine-induced contraction in Ca^{2+}-free solution was then compared to the contractions in the presence or absence of levobunolol. Levobunolol significantly reduced the histamine-induced contraction in Ca^{2+}-free medium ($^*P < 0.05$, $n = 22$). The amplitude of contraction induced by high-K solution was defined as 100%. The vertical bar with 1mN represents the actual isometric tension of rabbit ciliary arteries in myograph system.

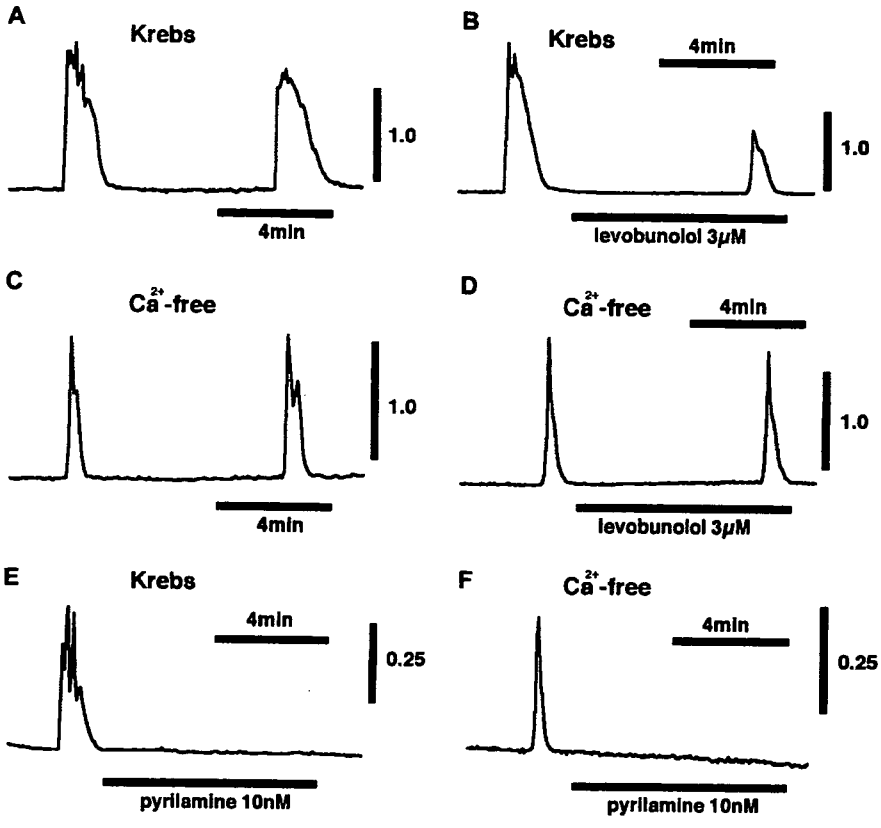

Fig. 6. Effects of levobunolol and pyrilamine on the histamine-induced increase of $[Ca^{2+}]_i$ in human aortic smooth muscle cells. Histamine (1 μM) was applied twice with a 7 min interval between application. Levobunolol (3 μM) or pyrilamine (10 nM) were pre-incubated before the second application of histamine. (A, B) In Krebs medium, levobunolol reduced the $[Ca^{2+}]_i$ in response to histamine. (C, D) In Ca^{2+}-free medium, levobunolol did not reduced the $[Ca^{2+}]_i$ in response to histamine. (E, F) Pyrilamine (10 nM) reduced the $[Ca^{2+}]_i$ in response to histamine in both Krebs medium and in Ca^{2+}-free medium. The vertical bar with either 1.0 or 0.25 represents the ratio of F_{340}/F_{380} which was monitored to determine the $[Ca^{2+}]_i$ in Aquacosmos System.

A or endothelin B receptors, it induces smooth muscle contraction by releasing Ca^{2+} from intracellular stores and promoting entry from the extracellular medium (Masaki, 2004).

Levobunolol was more effective on histamine-induced contractions compared to others. However, its relaxation effect is unlikely to be mediated through the H_1 receptor because levobunolol does not displace [^{3}H]pyrilamine binding to that receptor. In the absence of any affinity for the H_1 receptor, levobunolol must antagonize the histamine-induced contraction through some other mechanism.

NO is formed from L-arginine by NO synthase in vascular endothelial cells and mediates the endothelium-dependent relaxation of vascular smooth muscle (Palmer et al., 1988). L-NAME, a NO synthase inhibitor, had no effect on the levobunolol-induced relaxation. Further, to investigate whether any endothelium-derived factor was involved in the relaxation mechanism, we denuded the vascular endothelium. This also had no effect on levobunolol-induced relaxation. These results suggested that NO or other endothelium-derived factors are not involved in the levobunolol relaxing mechanism.

In the present studies, phenylephrine, an α_1-adrenergic agonist, induced concentration-dependent contractions in rabbit ciliary artery. Levobunolol may have some α_1-antagonistic action in addition to the well known β-antagonistic action (Mitsuoka et al., 1997). However, levobunolol only depressed the phenylephrine concentration–response curve and did not shift this curve to the right. Therefore, it seems that the α_1-adrenergic receptor does not participate in the relaxant effect of levobunolol.

It has been reported that levobunolol inhibits the intracellular Ca^{2+} increases by blocking the L-type voltage-dependent Ca^{2+} channel (Wu et al., 2004). In present studies, we found that levobunolol was more effective in relaxing the histamine-induced contraction compared to the high-K-induced contraction. On the other hand, diltiazem, a typical L-type voltage-dependent Ca^{2+} channel blocker (Gunthorpe and Lummis, 1999), had a greater effect on the high-K-induced contraction. Diltiazem blocks L-type voltage-dependent Ca^{2+} channels, but these channels were not blocked by levobunolol in our cultured human aortic smooth muscle cells, though at higher concentrations they may do so. These differences between levobunolol and diltiazem suggest that the relaxing mechanism of levobunolol is different from that of diltiazem.

Our fluorescence photometry studies using cultured human aortic smooth muscle cells indicated that levobunolol

Table 2
Inhibitory effects of levobunolol or pyrilamine on histamine-induced increase of $[Ca^{2+}]_i$

Incubation medium	Control	3 μM Levobunolol	10 nM Pyrilamine
Krebs solution	72.5 ± 6.9 (35)	45.9 ± 18.9* (41)	20.8 ± 30.3* (27)
Ca^{2+}-free solution	83.5 ± 9.2 (34)	99.8 ± 37.0 (35)	15.3 ± 23.8* (28)

The amplitude of $[Ca^{2+}]_i$ induced by the first application of 1 μM histamine was defined as 100%. Values were expressed as per cents of $[Ca^{2+}]_i$ in the first application. *$P < 0.05$ compared to control.

decreased the $[Ca^{2+}]_i$ that was elevated by histamine in Ca^{2+}-containing Krebs solution, but it had no effect in Ca^{2+}-free solution. Thus, we conclude that the relaxation mechanism of levobunolol is partly due to the blocking of extracellular Ca^{2+} entry through non-voltage-dependent Ca^{2+} channels. These data also suggest that levobunolol does not inhibit Ca^{2+} release from intracellular stores. However, levobunolol did inhibit the rabbit ciliary artery contraction induced by histamine in Ca^{2+}-free solution. These apparent discrepancies may be due to species-specific differences in smooth muscle physiology. They may also be due to differences in the responsiveness of cultured cells compared to in situ cells.

Pyrilamine, a histamine H_1 antagonist, relaxed histamine pre-contracted preparations, and it also strongly inhibited the histamine-induced increase of $[Ca^{2+}]_i$ in the cultured human aortic smooth muscle cells in both Ca^{2+}-containing Krebs and in Ca^{2+}-free solution. This suggests that levobunolol, which did not affect $[Ca^{2+}]_i$ in Ca^{2+}-free media, induces relaxation by changing Ca^{2+} sensitivity or by other intracellular Ca^{2+} independent mechanisms.

In summary, the vasodilatory mechanism of levobunolol was independent of NO or vascular endothelium, and it was not dependent on α_1-adrenergic receptor antagonism. Moreover, levobunolol did not have histamine receptor antagonistic action. We conclude that levobunolol relaxes rabbit ciliary artery by two different mechanisms. First, the relaxation may be due to the blockade of Ca^{2+} entry through non-voltage-dependent Ca^{2+} channels. Second, levobunolol may induce relaxation by intracellular Ca^{2+}-independent mechanisms. These actions of levobunolol may explain the mechanisms of increased ocular blood flow in vivo.

Acknowledgments

The authors thank Kaken Pharm Co. for providing levobunolol for these experiments, and Ms. Sanae Takaseki for her excellent technical assistance. Supported by Japan Society for the Promotion of Science Grant-in-Aid for Scientific Research #12671718 and 12671719.

References

Arend, O., Harris, A., Arend, S., Remky, A., Martin, B.J., 1998. The acute effect of topical beta-adrenoreceptor blocking agents on retinal and optic nerve head circulation. Acta Ophthalmol. Scand. 76, 43–49.

Bosem, M.E., Lusky, M., Weinreb, R.N., 1992. Short-term effects of levobunolol on ocular pulsatile flow. Am. J. Ophthalmol. 114, 280–286.

Chiou, G.C., Zhao, F., Shen, Z.F., Li, B.H., 1990. Effects of D-timolol and L-timolol on ocular blood flow and intraocular pressure. J. Ocul. Pharmacol. 6 (1), 23–30.

Collignon-Brach, J., 1994. Longterm effect of topical beta-blockers on intraocular pressure and visual field sensitivity in ocular hypertension and chronic open-angle glaucoma. Surv. Ophthalmol. 38, S149–S155.

Drance, S.M., 1998. A comparison of the effects of betaxolol, timolol, and pilocarpine on visual function in patients with open-angle glaucoma. J. Glaucoma. 7, 247–252.

Eckert, R.E., Karsten, A.J., Utz, J., Ziegler, M., 2000. Regulation of renal artery smooth muscle tone by α_1-adrenoceptors: role of voltage-gated calcium channels and intracellular calcium stores. Urol. Res. 28, 122–127.

Flammer, J., 1994. The vascular concept of glaucoma. Surv. Ophthalmol. 38, S3–S6.

Georgopoulos, G.T., Diestelhorst, M., Fisher, R., Ruokonen, P., Krieglstein, G.K., 2002. The short-term effect of latanoprost on intraocular pressure and pulsatile ocular blood flow. Acta Ophthalmol. Scand. 80, 54–58.

Grunwald, J.E., 1990. Effect of timolol maleate on the retinal circulation of human eyes with ocular hypertension. Invest. Ophthalmol. Vis. Sci. 31, 521–526.

Gunthorpe, M.J., Lummis, S.C., 1999. Diltiazem causes open channel block of recombinant 5-HT3 receptors. J. Physiol. 519, 713–722.

Gustafsson, H., 1993. Vasomotion and underlying mechanisms in small arteries. An in vitro study of rat blood vessels. Acta Physiol. Scand. Suppl. 614, 1–44.

Hayashi-Morimoto, R., Yoshitomi, T., Ishikawa, H., Hayashi, E., Sato, Y., 1999. Effects of beta antagonists on mechanical properties in rabbit ciliary artery. Graefes Arch. Clin. Exp. Ophthalmol. 237, 661–667.

Highsmith, R.F., Pang, D.C., Rapoport, R.M., 1989. Endothelial cell-derived vasoconstrictors: Mechanisms of action in vascular smooth muscle. J. Cardiovasc. Pharmacol. 13 (Suppl 5), S36–S44.

Ishikawa, H., Yoshitomi, T., Mashimo, K., Nakanishi, M., Shimizu, K., 2002. Pharmacological effects of latanoprost, prostaglandin E2, and F2α on isolated rabbit ciliary artery. Graefes Arch. Clin. Exp. Ophthalmol. 240, 120–125.

Keef, K.D., Bowen, S.M., 1989. Effect of ACh on electrical and mechanical activity in guinea pig coronary arteries. Am. J. Physiol. 257, H1096–H1103.

Kimura, I., Shinoda, K., Tanino, T., Ohtake, Y., Mashima, Y., 2005. Effect of topical unoprostone isopropyl on optic nerve head circulation in controls and in normal-tension glaucoma patients. Jpn. J. Ophthalmol. 49, 287–293.

Laporte, R., Laher, I., 1997. Sarcoplasmic reticulum-sarcolemma interactions and vascular smooth muscle tone. J. Vasc. Res. 34, 325–343.

Masaki, T., 2004. Historical review: Endothelin. Trends Pharmacol. Sci. 25, 219–224.

Mitsuoka, Y., Matsuzawa, S., Tachiiri, T., Momo, K., 1997. Effects of AG-901 ophthalmic solution on intraocular pressure in ocular hypertensive rabbits and ocular blood flow in ocular normotensive rabbits. Atarashii Ganka 14, 801–806.

Morsman, C.D., Bosem, M.E., Lusky, M., Weinreb, R.N., 1995. The effect of topical beta-adrenoceptor blocking agents on pulsatile ocular blood flow. Eye 9, 344–347.

Mulvany, M.J., Halpern, W., 1976. Mechanical properties of vascular smooth muscle cells in situ. Nature 260, 617–619.

Mulvany, M.J., Halpern, W., 1977. Contractile properties of small arterial resistance vessels in spontaneously hypertensive and normotensive rats. Circ. Res. 41, 19–26.

Murakawa, K., Kohno, M., Yokokawa, K., Yasunari, K., Horio, T., Kurihara, N., Takeda, T., 1990. Endothelin-induced renal vasoconstriction and increase in cytosolic calcium in renal vascular smooth muscle cell. Clin. Exp. Hypertens. A. 12, 1037–1048.

Nguyen, T., Shapiro, D.A., George, S.R., Setola, V., Lee, D.K., Cheng, R., Rauser, L., Lee, S.P., Lynch, K.R., Roth, B.L., Odowd, B.F., 2001. Discovery of a novel member of the histamine receptor family. Mol. Pharmacol. 59, 427–433.

Ogasawara, H., Yoshida, A., Fujio, N., Konno, S., Ishiko, S., 1999. Effect of topical levobunolol on retinal, optic nerve head, and choroidal circulation in normal volunteers. Nippon Ganka Gakkai Zasshi 103, 544–550.

Palmer, R.M., Rees, D.D., Ashton, D.S., Moncada, S., 1988. L-Arginine is the physiological precursor for the formation of nitric oxide in endothelium-dependent relaxation. Biochem. Biophys. Res. Commun. 153, 1251–1256.

Sato, T., Muto, T., Ishibashi, Y., Roy, S., 2001. Short-term effect of beta-adrenoreceptor blocking agents on ocular blood flow. Curr. Eye Res. 23 (4), 298–306.

Setoguchi, M., Ohya, Y., Abe, I., Fujishima, M., 1995. Inhibitory action of betaxolol, a beta 1-selective adrenoceptor antagonist, on voltage-dependent calcium channels in guinea-pig artery and vein. Br. J. Pharmacol. 115 (1), 198–202.

Shaikh, M.H., Mars, J.S., 2001. The acute effect of pilocarpine on pulsatile ocular blood flow in ocular hypertension. Eye 15, 63–66.

Wu, K.Y., Wang, H.Z., Hong, S.J., 2004. Inhibition of endothelin-1 and KCl-induced increase of $[Ca^{2+}]_i$ by antiglaucoma drugs in cultured A7r5 vascular smooth-muscle cells. J. Ocul. Pharmacol. Ther. 20, 201–209.

Yoshitomi, T., Ishikawa, H., Hayashi, E., 2000. Pharmacological effects of pilocarpine on rabbit ciliary artery. Curr. Eye Res. 20, 254–259.

Yoshitomi, T., Yamaji, K., Ishikawa, H., Ohnishi, Y., 2002. Vasodilatory effects of nipradilol, an alpha- and beta-adrenergic blocker with nitric oxide releasing action, in rabbit ciliary artery. Exp. Eye Res. 75, 669–676.

Yoshitomi, T., Yamaji, K., Ishikawa, H., Ohnishi, Y., 2004. Vasodilatory mechanism of unoprostone isopropyl on isolated rabbit ciliary artery. Curr. Eye Res. 28, 167–174.

Available online at www.sciencedirect.com
ScienceDirect
Experimental Eye Research 84 (2007) 626–634
EXPERIMENTAL EYE RESEARCH
www.elsevier.com/locate/yexer

Existence of small slow-cycling Langerhans cells in the limbal basal epithelium that express ABCG2

Wensheng Chen [a,b], Koji Hara [b], Qing Tian [c], Kanxing Zhao [a,*], Takeshi Yoshitomi [b]

[a] *Tianjin Medical University, Tianjin Eye Hospital, Tianjin, China*
[b] *Department of Ophthalmology, Akita University School of Medicine, Hondo 1-1-1, Akita 010, Japan*
[c] *Nanyang Eye Hospital, City of Nanyang, Henan Province, China*

Received 26 July 2006; accepted in revised form 13 November 2006
Available online 23 January 2007

Abstract

Despite the obvious importance of limbal stem cells in corneal homeostasis and tumorigenesis, little is known about their specific biological characteristics. The purpose of this study was to characterize limbal slow-cycling cells based on the expression of ABCG2 and major histocompatibility complex (MHC) class II and the cell size. Wistar rats were daily injected with 5-bromo-2-deoxyuridine (BrdU) at a dose of 5 mg/100 g for 2 weeks. After 4-week BrdU-free period, corneal tissues were excised, and immunofluorescence staining for ABCG2, BrdU, and MHC class II was performed by confocal microscopy. In another series, corneal tissues of normal rat were double immunostained for ABCG2, keratin 14, keratin 3, CD11c, and MHC class II. In addition, limbal, peripheral and central corneal epithelial sheets were isolated by Dispase II digestion and dissociated into single cell by trypsin digestion and cytospin preparations were double immunostained for ABCG2 and MHC class II. The cell size and nucleus-to-cytoplasm (N/C) ratio of limbal ABCG2$^+$ cells were analyzed and compared with those of cells from other zones. BrdU label-retaining cells (LRCs) with expression of ABCG2 were found in the limbal epithelial basal layer, but not in other parts of the cornea. Approximately 20% of these cells were MHC class II positive. All MHC class II$^+$ cells in the corneal epithelium were positive for CD11c, a marker for dendritic cells (DCs). Double labeling with ABCG2 and keratin 14 showed that nearly four-fifth of limbal ABCG2$^+$ cells were positive for keratin 14 but negative for keratin 3, exhibiting an undifferentiated epithelial cell lineage. Cytospin sample analysis revealed the presence of a distinct population of smaller ABCG2$^+$ cells with expression of MHC class II with a larger N/C ratio in the limbal epithelium. A new population of small slow-cycling cells with large N/C ratio has been found to express ABCG2 in the limbal epithelial basal layer. Some of these cells normally express MHC class II antigen. These findings may have important implications for our understanding of the characteristics of limbal slow-cycling cells.

Keywords: limbal stem cell; slow-cycling cells; ABCG2; major histocompatibility complex class II; CD11c; Langerhans cell

1. Introduction

It is easy to be fascinated by limbal stem cells, not only because they play a pivotal role in corneal epithelial homeostasis and tumorigenesis, but also because they are exclusively concentrated in the limbal epithelial basal layer and are completely separated from their progeny cells, transient amplifying (TA) cells in the peripheral and central corneal epithelia. Such a compartmentalization of limbal stem cells provides an excellent model for studying the growth and differentiation of stem cells and TA cells. As yet, corneal epithelial stem cells have been detected in the limbal epithelial basal layer by determination of slow-cycling cells (label-retaining cells [LRCs]) by mitotic DNA labeling (Cotsarelis et al., 1989; Lavker et al., 1991; Chen et al., 2003), comparison of proliferative capacity in vivo and in vitro (Ebato et al., 1988; Lavker et al., 1998; Hernandez Galindo et al., 2003), comparison of

* Corresponding author. Present address: Tianjin Eye Hospital, No 4, Gansu Road, Heping District, Tianjin 300020, People's Republic of China. Tel: +86 22 27313336; fax: +86 22 27313133.
E-mail address: ZKX@tijmu.edu.cn (K. Zhao).

0014-4835/$ - see front matter © 2006 Elsevier Ltd. All rights reserved.
doi:10.1016/j.exer.2006.11.006

cell size and nucleus-to-cytoplasm (N/C) ratios (Romano et al., 2003; Arpitha et al., 2005), and expression of some polypeptides (Schlötzer-Schrehardt and Kruse, 2005).

Recently, for the identification of limbal stem cells, a number of investigations have been performed to examine the expression of ABCG2, a member of the ATP binding cassette (ABC) transporters, in the corneal epithelium. Different from most other putative markers for limbal stem cells that label the majority of limbal basal cells, ABCG2 expression is strictly confined to small clusters of basal cells in the limbal epithelium (Chen et al., 2004; Umemoto et al., 2005; de Paiva et al., 2005). Furthermore, limbal ABCG2$^+$ cells grow better than limbal ABCG2$^-$ cells in human cell culture (de Paiva et al., 2005). Therefore, ABCG2 has been considered to be the only maker that is able to distinguish limbal stem cells from TA cells and the most useful cell surface marker for the identification and isolation of limbal stem cells (Schlötzer-Schrehardt and Kruse, 2005).

Although these findings are consistent with the fact that corneal epithelial stem cells are exclusively located in the limbal basal epithelium, no direct evidence is yet available to confirm that limbal ABCG2$^+$ cells are epithelial stem cells, because limbal basal epithelium also contains TA cells, and as well as a small number of Langerhans cells (LCs) and melanocytes (Cotsarelis et al., 1989; Higa et al., 2005). Even more important, the label-retaining property of limbal ABCG2$^+$ cells has never been directly demonstrated.

Under normal condition, limbal stem cells are slow-cycling, that is, cells endowed with a long cell time (which indicates low mitotic activity). Therefore, the identification of these cells can be based on the presence of thymidine or 5-bromo-2-deoxyuridine (BrdU) LRCs (Lehrer et al., 1998; Nagasaki and Zhao, 2005). In the present study, we characterized limbal slow-cycling cells based on the expression of ABCG2 and histocompatibility complex (MHC) class II molecules. We found that all limbal ABCG2$^+$ cells are smaller slow-cycling cells with large N/C ratio. We show that the uninflamed limbal basal epithelium is endowed with a small number of slow-cycling LCs with expression of ABCG2. The significance of the findings is further discussed.

2. Materials and methods

BrdU-labeling reagent was purchased from Zymed Laboratories (South San Francisco, CA, USA); pentobarbital sodium from Abbott Laboratories (North Chicago, IL, USA); Dulbecco modified Eagle medium (DMEM), Dispase II, 0.25% Trypsin-0.02% EDTA, and 5% FBS–HBSS from Invitrogen Corp (Carlsbad, CA); fetal bovine serum (FBS) from HyClone (Logan, UT); biotinylated mouse anti-BrdU antibody (BrdU-labeling kit) from Oncresprod (Boston, MA, USA); FITC-conjugated MHC class II antibody (OX6) from Immunotech (Marseille, France); biotinylated mouse monoclonal anti-rat MHC class II monoclonal antibody (RT1B; OX6) from PharMingen (San Diego, CA); FITC-conjugated anti-ABCG2 antibody (5D3) from MBL (Aichi, Japan); biotinylated mouse monoclonal anti-rat keratin 14 (clone LL002) and keratin 3 from Lab Vision (Fremont, CA); mouse anti-rat CD11c from Cosmobio (Tokyo, Japan); rhodamine-conjugated goat anti-mouse IgG from Biochemical Division (Aurora, Ohio); streptavidin-conjugated Alexa Fluor 594 and streptavidin-conjugated Alexa Fluor 350 from Molecular Probes (Eugene, OR); 4,6-diamidino-2-phenylindole (DAPI) and normal goat serum from Vector Laboratories (Burlingame CA).

2.1. Experimental animals

A total of 30 six-week-old Wistar rats of either sex were used in the study. The animals were housed in individual cages at constant room temperature (19–23 °C) and humidity of 40–50%, and with a constant 12-h light–dark cycle (Animal House, University of Akita, Japan). Before any experimental procedure, the animals were examined for ocular surface disease with handheld biomicroscope and were excluded if any disease was found. All subsequent experiments were conducted in accord with the ARVO statement for the use of Animals in Ophthalmic and Vision Research and received the approval of the Animal Care Facility of Akita University School of Medicine.

2.2. Labeling of slow-cycling cells

To label slow-cycling stem cells, 10 rats received daily injection of BrdU for 2 weeks at a dose of 5 mg/100 g. The animals were left untreated for 4 weeks. Following this chase period, only slow-cycling stem cells retained their label and could be identified by the presence of BrdU LRCs (Lehrer et al., 1998).

2.3. Preparation of cytospin sample

After being killed with an overdose of pentobarbital sodium, corneas were excised from normal rats ($n = 5$). Central cornea was punched out using a 2-mm trephine. Limbal rim was separated from sclera and peripheral cornea using a scalpel under the stereomicroscope. Limbal, peripheral and central corneal tissues were treated with Dispase II (2 mg/mL in DMEM) at 37 °C for 45 min. Epithelial sheet was then removed and treated with 0.25% trypsin/1 mM EDTA solution to harvest dissociated cells. After centrifugation at 780 × g for 10 min, cells were resuspended in DMEM containing 10% FBS to stop enzyme activity. After being washed in PBS, cell suspension was filtered through a 40 μm Cell Strainer (BD Falcon, San Jose, CA) to collect single cell. After centrifugation at 400 × g for 5 min, cells for cytospin preparation (5.0×10^4 cells/slide) were deposited on glass slides using Auto Smear CF-12D (Sakura Finetek, Tokyo, Japan).

2.4. Immunohistochemical studies

After BrdU LRCs containing eyes ($n = 20$) had been enucleated and fixed in PBS with 1% paraformaldehyde for 24 h, under a dissecting microscope (Model SZ40; Olympus, Tokyo, Japan), the retina, lens, and iris were discarded, and four incisions were made in each cornea. Subsequently, the

corneas were washed in PBS with 1% Triton X-100 and 1% dimethyl sulfoxide (DMSO; TD buffer). To block nonspecific staining, corneas were incubated in 1.5% normal goat serum diluted in TD buffer for 1 h. Then, the tissues were incubated with either FITC-conjugated anti-ABCG2 antibody or FITC-conjugated anti-rat MHC class II antibody overnight with agitation (50 turns per minute). The second day, the tissues were washed with distilled water, placed in 0.3 N HCl for 30 min, washed in TD buffer. Next, the tissues were incubated in blocking solution for 1 h. Afterward, the tissues were incubated in biotinylated anti-BrdU antibody for 4 h with agitation. The tissues were then rinsed with TD buffer and placed in streptavidin-conjugated Alexa Fluor 594 for 2 h with agitation. After distilled water wash, the whole-mount cornea tissues were mounted epithelial side up on a slide and stained with a nuclear fluorescence dye, DAPI.

To determine whether limbal ABCG2$^+$ cells express keratin 14 and keratin 3, immunostaining of normal corneal tissues ($n = 30$) for ABCG2, keratin 14, and keratin 3 was performed. Briefly, after being washed in TD buffer, the tissues were incubated in blocking solution for 1 h. Then, a mixture of FITC-conjugated anti-ABCG2 antibody and biotinylated anti-rat keratin 14 (or keratin 3) was applied to the tissues overnight. The next day, they were washed in TD buffer and placed in streptavidin-conjugated Alexa Fluor 350 for 2 h. DAPI was used as a DNA counterstain.

Double staining of normal corneal tissues with CD11c and MHC class II was also performed to determine whether MHC class II$^+$ cells expressed dendritic cell (DC)/LC marker (Camelo et al., 2004). Briefly, corneal tissues were washed in TD buffer and incubated in blocking solution. Then, a mixture of FITC-conjugated anti-rat MHC class II antibody and mouse anti-rat CD11c antibody was applied to the samples overnight. The next day, the tissues were washed in TD buffer and rhodamine-conjugated goat affinity purified anti-mouse IgG was applied to the sample for 2 h, followed counterstaining with DAPI. All incubations were performed at RT. All antibodies were optimally diluted in TD buffer.

All the corneal tissues that had been observed on whole mount were snap-frozen in liquid nitrogen, and 10 μm thick cross-sections were prepared with cryostat. These sections were also examined by confocal microscopy.

Double staining of cytospin preparations separated from normal corneas for MHC class II and ABCG2 were performed to determine the ABCG2$^+$ cells with expression of MHC class II. Briefly, after being washed in PBS, blocking solution was applied to the cytospin preparations for 30 min. The cytospin preparations were then incubated in a mixture of FITC-conjugated anti-ABCG2 antibody and biotinylated anti-rat MHC class II antibody for 1 h. Then, the cytospin preparations were rinsed with PBS and placed in diluted streptavidin-conjugated Alexa Fluor 594. DAPI was used as a DNA counterstain.

2.5. Confocal microscopy

A confocal laser scanning microscopy (LSM510 Axiovert200M; Carl Zeiss Meditec, Göttingen, Germany) was used to image the localization of DAPI (405-nm laser line excitation; 420/80 emission filter), Alexa 488 (488-nm laser line excitation; 505/530 emission filter) and Alexa 594 (594-nm laser line excitation; 560/593 emission filter). Images were captured with identical photomultiplier tube gain setting and processed (LSM-PC; Carl Zeiss Meditec, Inc), using the Z-stack option. Multiple scans from the surface to the basal layer of the corneal epithelium can be obtained by this technique. The rat cornea, which has a diameter of 7 mm, was divided into three different areas. The central cornea was defined as the area within 2 mm of the corneal center. The peripheral cornea was the area between 2 mm of the center and the semi-transparent limbus viewed under transmitted light. The limbus was the area between peripheral cornea and presence of goblet cells in flat whole mounts. Using grid, the number of cells with different markers in surface and basal layers of different epithelial zones was counted. At least five different areas were observed in each sample. Values were expressed as the mean ± SEM of the cells/mm^2. Images were reproduced for publication with image-management software (Photoshop 7.0; Adobe Systems Inc., Mountain View, CA).

Cellular and nuclear areas of single cell in cytospin preparations were measured using the confocal software (LSM Image Browser). Briefly, fluorescence Z-stack (1-μm) images were obtained simultaneously for FITC and Alexa Fluor 594 and DAPI and transmitted light for 50 limbal ABCG2$^+$ cells with expression of MHC class II, limbal ABCG2$^+$ cells without expression of MHC class II, peripheral, and central corneal epithelial cells. The polygon tool from stack was used to draw the region of interest (ROI) around the cell in the transmitted light image and the ROI around the DAPI-stained region for the nuclear area of the same cell.

2.6. Statistical analysis

Fifty cells from the limbal, peripheral and central corneal epithelia were chosen for cell and nuclear areas measurement. N/C ratio was created by dividing the area of nuclear with that of the cell. The Mann–Whitney U test was used to compare mean values. A value of $P < 0.05$ was considered significant.

3. Results

3.1. Distribution of BrdU LRCs in the corneal epithelium

After rats were injected with BrdU daily for 2 weeks, immunohistochemical analysis was performed to determine BrdU-labeled cells in the corneal epithelium. Staining with BrdU antibody revealed that, 14 days after injection of BrdU, over 80% of central corneal epithelial cells, over 75% of peripheral corneal epithelial cells, and over 70% of limbal epithelial cells were BrdU-labeled. After a 4-week BrdU-free period, all of the BrdU-labeled cells disappeared from central and peripheral cornea. However, the limbal basal epithelium was populated with a number of round BrdU-labeled cells (43 ± 10.3cells/mm^2) (Fig. 1).

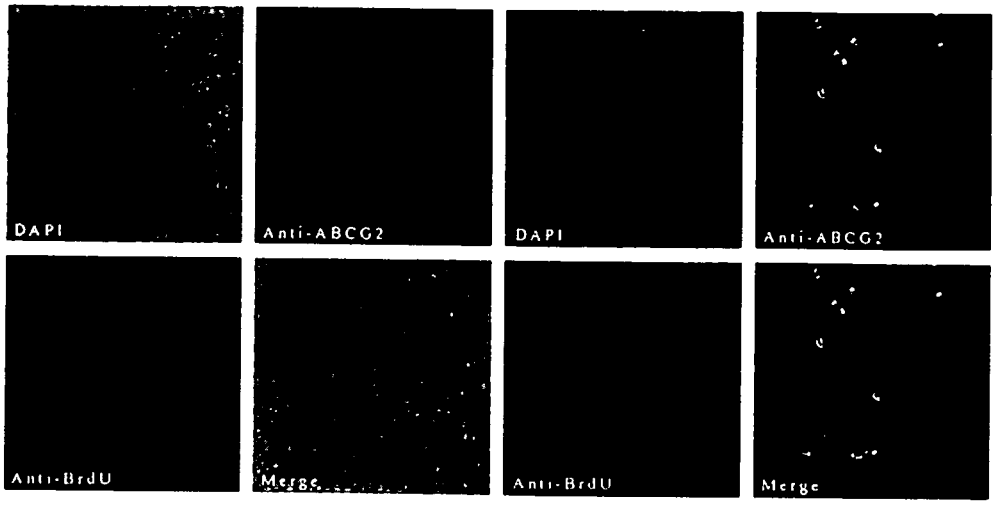

Fig. 1. Distribution of slow-cycling cells in rat corneal epithelium. (left) Peripheral corneal basal epithelium; (right) limbal basal epithelium. After daily injection of BrdU followed by 1-month BrdU-free period, the slow-cycling BrdU-labeled cells are localized in the limbal basal epithelium. Double staining with ABCG2 antibody showed that all BrdU LRCs expressed ABCG2 (pink). In contrast, no such cells can be found in peripheral corneal basal epithelium.

3.2. Expression of ABCG2, MHC class II molecules, CD11c, keratin 14 and keratin 3 in the corneal epithelium

Immunofluorescence labeling of corneal tissues with ABCG2 antibody revealed that ABCG2$^+$ cells were located in the limbal basal epithelium. Double staining of corneal tissues with BrdU antibody showed that the same cells were positive for BrdU label-retaining test. In contrast, there was no expression of ABCG2 in the peripheral and central corneal basal epithelium (Fig. 1). To determine the location of BrdU LRC with expression of ABCG2 within the epithelium, the corneal tissues were stained with a nuclear dye, DAPI, which help to discriminate basal epithelium from surface epithelium based on the density of the nuclei. As previously reported in mouse cornea, the density of the peripheral and central surface epithelial cell nuclei was lower than that of basal epithelial cells (Nagasaki and Zhao, 2003). In limbus, however, the density of surface epithelial cell was higher than that of basal epithelial cells. To further confirm the vertical location of limbal BrdU LRC, cryosections were prepared from whole-mount cornea tissues whose en face profile had been examined previously. This method made a direct comparison between an en face view and a cross-sectional view of the same cells. The results revealed that all limbal BrdU LRCs with expression of ABCG2 were located in the limbal epithelial basal layer (data not showed).

Immunofluorescence labeling of corneal tissues with MHC class II antibody showed expression of MHC class II only at the limbus (96 ± 7.8 cells/mm^2) and periphery (87 ± 2.7 cells/mm^2) of the cornea, whereas the cells in the central epithelium were all negative for MHC class II. In the limbal and peripheral corneal surface epithelia, dendrite-shaped MHC class II$^+$ cells formed a dense collar around the cornea. Simultaneous staining of BrdU LRCs containing corneal tissues with BrdU antibody revealed that these cells were all negative for BrdU labeling, whereas approximately 20% of limbal BrdU LRCs expressed MHC class II antigen (Fig. 2). This finding was confirmed by cross-sectional studies, which showed that MHC class II$^+$ BrdU-labeled cells were exclusively located in the limbal epithelial basal layer (Fig. 3). Double labeling with CD11c showed that all the MHC class II$^+$ cells in the limbal basal epithelium were positive for CD11c (Fig. 4).

Immunofluorescence labeling of corneal tissues with keratin 3 and keratin 14 revealed that keratin 14$^+$ cells were localized in the limbal and peripheral basal epithelia, while keratin 3$^+$ cells were primarily concentrated in the central area. Double staining of corneal tissues with ABCG2 and keratin 14 showed that nearly four-fifth of limbal ABCG2$^+$ cells expressed K14 (Fig. 4).

3.3. Cytospin sample analysis

As our results suggested that limbal ABCG2$^+$ cells are slow-cycling cells, we next performed double immunofluorescence staining of cytospin sample to determine the cell size and N/C ratio of these cells. Immunostaining of cytospin preparations with ABCG2 showed that of all cells isolated from normal limbal epithelium, ABCG2$^+$ cells comprised an average of $2.6 \pm 0.7\%$. Double staining with MHC class II revealed that nearly one-fifth of limbal ABCG2$^+$ cells expressed MHC class II antigen (Fig. 5). All the size of limbal ABCG2$^+$ cells was significantly smaller, whereas the N/C ratio of these cells was significantly larger than those of peripheral and central corneal epithelial cells (Table 1). However, there was no significant difference between limbal ABCG2$^+$ cells with expression of MHC class II and limbal ABCG2$^+$ cells without expression of MHC.

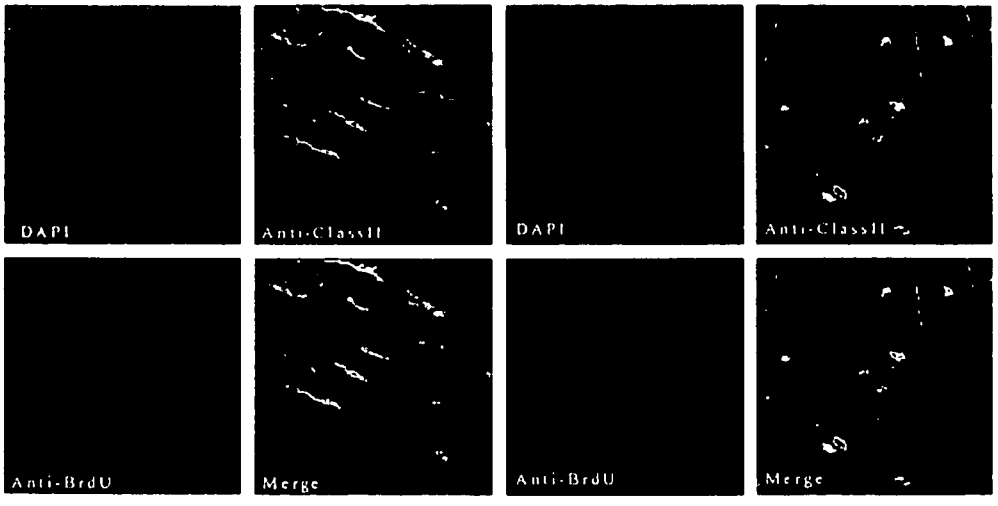

Fig. 2. Distribution of BrdU-labeled and MHC class II^+ cells in the limbal epithelium. (left) Limbal surface epithelium; (right) limbal basal epithelium. Whole-mount corneal tissues were assessed for BrdU labeling and expression of MHC class II antigen in the limbal epithelium. Confocal micrographs show significant number of dendrite-type MHC class II^+ cells in the surface epithelium of the limbus. These cells were all negative for BrdU labeling. In contrast, a number of round MHC class II^+ cells were present in the limbal basal epithelium and some of them were positive for BrdU labeling (pink). Note that the density of the limbal surface epithelial cells was higher than that of the limbal basal epithelial cells.

4. Discussion

As expected, BrdU LRCs were found to be exclusively concentrated in the limbal basal epithelium. Previous studies in mouse (Cotsarelis et al., 1989), rabbit (Wirtschafter et al., 1999), and rat (Chen et al., 2003) have demonstrated that slow-cycling cells are concentrated in the basal epithelium of the limbus but are absent from the peripheral and central corneal epithelia. Existence of slow-cycling cells in the limbal epithelium, on the one hand, coupled with the failure to routinely detect slow-cycling cells in other corneal epithelium on the other, has led to the conclusion that corneal epithelial stem cells are exclusively located in the limbus. The present study indicates that approximately $2.6 \pm 0.7\%$ of limbal epithelial cells can be identified as BrdU LRCs with expression of ABCG2. This finding is in accordance with another study reporting that corneal stem cells represent less 10% of the total limbal basal cell population (Lavker et al., 1991).

ABCG2, a member of ABC transporters, formally known as breast cancer resistance protein 1, is expressed in a wide variety of primitive stem cells (Trosko and Ruch, 1998; Zhou et al., 2001; Kim and Turnquist, 2002). Constitutive expression of ABCG2 is thought to be associated with the side population (SP) phenotype based on the ability to efflux Hoechst

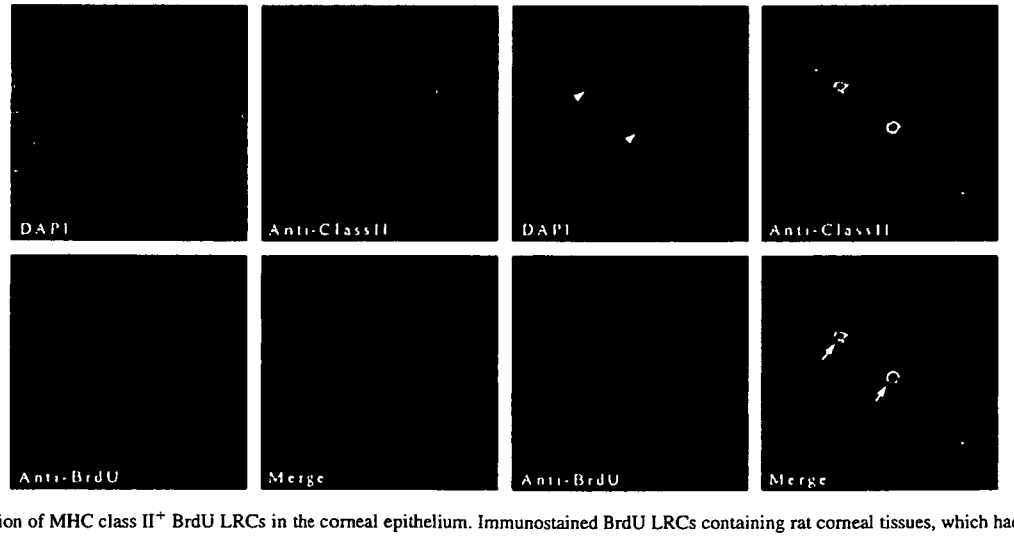

Fig. 3. Localization of MHC class II^+ BrdU LRCs in the corneal epithelium. Immunostained BrdU LRCs containing rat corneal tissues, which had been observed on whole mount, were cut into cross-sections and examined by confocal microscopy. (left) Central corneal epithelium; (right) limbal epithelium. Note that MHC class II^+ BrdU LRCs (arrow) are located in the limbal basal epithelium and the nuclei (arrowhead) of these cells are smaller compared with other limbal epithelial basal cells. In contrast, no such cells can be found in the central corneal epithelium.